Miner Deposita
DOI 10.1007/s00126-007-0126-6

ARTICLE

Petrology, geochemistry and U–Pb geochronology of magmatic rocks from the high-sulfidation epithermal Au–Cu Chelopech deposit, Srednogorie zone, Bulgaria

Isabelle Chambefort · Robert Moritz · Albrecht von Quadt

Received: 4 April 2006 / Accepted: 9 December 2006

Abstract The Chelopech deposit is one of the largest European gold deposits and is located 60 km east of Sofia, within the northern part of the Panagyurishte mineral district. It lies within the Banat–Srednegorie metallogenic belt, which extends from Romania through Serbia to Bulgaria. The magmatic rocks define a typical calc-alkaline suite. The magmatic rocks surrounding the Chelopech deposit have been affected by propylitic, quartz–sericite, and advanced argillic alteration, but the igneous textures have been preserved. Alteration processes have resulted in leaching of Na_2O, CaO, P_2O_5, and Sr and enrichment in K_2O and Rb. Trace element variation diagrams are typical of subduction-related volcanism, with negative anomalies in high field strength elements (HFSE) and light element, lithophile elements. HFSE and rare earth elements were relatively immobile during the hydrothermal alteration related to ore formation. Based on immobile element classification diagrams, the magmatic rocks are andesitic to dacitic in compositions. Single zircon grains, from three different magmatic rocks spanning the time of the Chelopech magmatism, were dated by high-precision U–Pb geochronology. Zircons of an altered andesitic body, which has been thrust over the deposit, yield a concordant $^{206}Pb/^{238}U$ age of 92.21±0.21 Ma. This age is interpreted as the crystallization age and the maximum age for magmatism at Chelopech. Zircon analyses of a dacitic dome-like body, which crops out to the north of the Chelopech deposit, give a mean $^{206}Pb/^{238}U$ age of 91.95± 0.28 Ma. Zircons of the andesitic hypabyssal body hosting the high-sulfidation mineralization and overprinted by hydrothermal alteration give a concordant $^{206}Pb/^{238}U$ age of 91.45±0.15 Ma. This age is interpreted as the intrusion age of the andesite and as the maximum age of the Chelopech epithermal high-sulfidation deposit. $^{176}Hf/^{177}Hf$ isotope ratios of zircons from the Chelopech magmatic rocks, together with published data on the Chelopech area and the about 92-Ma-old Elatsite porphyry–Cu deposit, suggest two different magma sources in the Chelopech–Elatsite magmatic area. Magmatic rocks associated with the Elatsite porphyry–Cu deposit and the dacitic dome-like body north of Chelopech are characterized by zircons with εHf_{T90} values of ~5, which suggest an important input of mantle-derived magma. Some zircons display lower εHf_{T90} values, as low as −6, and correlate with increasing $^{206}Pb/^{238}U$ ages up to about 350 Ma, suggesting assimilation of basement rocks during magmatism. In contrast, zircon grains in andesitic rocks from Chelopech are characterized by homogeneous $^{176}Hf/^{177}Hf$ isotope ratios with εHf_{T90} values of ~1 and suggest a homogeneous mixed crust–mantle magma source. We conclude that the Elatsite porphyry–Cu and the Chelopech high-sulfidation epithermal deposits were formed within a very short time span and could be partly contemporaneous. However, they

Editorial handling: B. Lehmann

I. Chambefort (✉) · R. Moritz
Section des Sciences de la Terre,
University of Geneva,
rue des Maraîchers 13,
1205 Geneva, Switzerland
e-mail: chambefi@geo.oregonstate.edu

Present address:
I. Chambefort
Department of Geosciences, Oregon State University
104 Wilkinson Hall,
Corvallis, OR 977331-5506, USA

A. von Quadt
Institute of Isotope Geology and Mineral Resources, ETH,
8092 Zurich, Switzerland

are related to two distinct upper crustal magmatic reservoirs, and they cannot be considered as a genetically paired porphyry–Cu and high-sulfidation epithermal related to a single magmatic–hydrothermal system centered on the same intrusion.

Keywords Chelopech · Au–Cu · High-sulfidation · Epithermal · Bulgaria · U–Pb dating · Hf isotopes

Introduction

The Bulgarian Panagyurishte mineral district is a major ore producing area within the Eastern European, Late Cretaceous Banat–Timok–Srednogorie belt (Berza et al. 1998; Ciobanu et al. 2002; Heinrich and Neubauer 2002). This district displays some of the best examples of porphyry–Cu and high-sulfidation epithermal ore deposit associations (Strashimirov et al. 2002; Moritz et al. 2004), more typically recognized in younger tectonic settings such as in the circum-Pacific region (Sillitoe 1997, 1999; Hedenquist and Lowenstern 1994; Corbett and Leach 1998). Within the northern Panagyurishte district, the high-sulfidation Au–Cu epithermal Chelopech deposit and the Elatsite porphyry–Cu deposit are two of the major producing mines and are only 6 km apart (Fig. 1). Based on their spatial relationship, they were interpreted as genetically linked (Popov et al. 2000, 2001; Strashimirov et al. 2002). We here examine the postulated genetic link of the magmatic rocks that host both deposits.

Only few geochronological studies, on Tertiary deposits, have documented the time relationships of spatially associated porphyry–Cu and high-sulfidation epithermal deposits. At Lepanto, Philippines (Arribas et al. 1995), adjacent porphyry–Cu and high-sulfidation epithermal deposits are coeval within resolution of radioisotopic age determinations. In contrast, at Mindanao, Philippines (Rohrlach 2003), La Famatina, Argentina (Losada-Calderòn et al. 1994; Losada-Calderòn and McPhail 1996), the Potrerillos district, Chile (Marsh et al. 1997), and the Emperor gold mine in the Tavua Caldera, Fiji (Setterfield et al. 1992), epithermal ore formation postdates exposed magmatism and porphyry–Cu ore formation by more than 1 Ma and by about 2 Ma at the Collahuasi district, northern Chile (Masterman et al. 2004, 2005), which is significantly longer than ≤100,000 years: The duration of a single

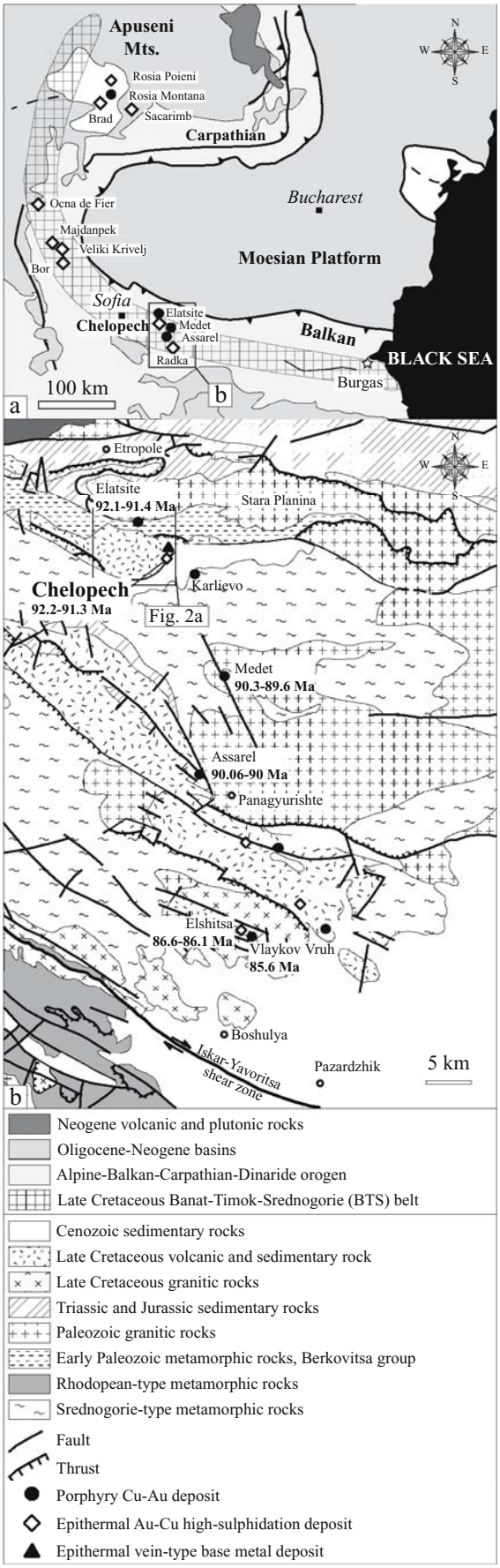

Fig. 1 **a** The Late Cretaceous Apuseni–Banat–Timok–Srednogorie (ABTS) belt (modified from Heinrich and Neubauer 2002). **b** Simplified geology of the Panagyurishte mineral district (after Cheshitev et al. 1995), U–Pb ages reported for the Panagyurishte deposits from von Quadt et al. (2005a), except Chelopech U–Pb ages from Stoykov et al. (2004)

hydrothermal event that can be sustained by a single upper crustal intrusion (Cathles et al. 1997).

In this contribution, we examine the time and genetic relationship of the Chelopech high-sulfidation epithermal deposit within the regional magmatic and metallogenic setting of the northern Panagyurishte district in light of new field observations, whole rock major and trace element compositions and precise U–Pb age data and Hf isotopic compositions of magmatic zircons.

Regional setting

The Chelopech deposit is one of the largest Au deposits in Europe. It is located in the northern part of the Panagyurishte mineral district (Popov and Popov 2000), which belongs to the Banat–Timok–Srednogorie belt (Fig. 1a). This tectonic zone is considered part of the Tethyan Eurasian metallogenic belt, which is linked to subduction magmatism during convergence of the African and Eurasian plates (Jankovic 1997; Berza et al. 1998; Ciobanu et al. 2002; Heinrich and Neubauer 2002; Lips 2002; von Quadt et al. 2005a,b), and is characterized by Late Cretaceous to Early Tertiary magmatic activity and ore formation. The Bulgarian part of this tectonic zone, the Srednogorie Belt, is subdivided into three magmatic segments: the Western, Central and Eastern Srednogorie zones. These zones are defined on the basis of the nature of the basement, the thickness of the crust, regional geophysical data, major element rock composition, and their petrological characteristics (Dabovski et al. 1991). The Panagyurishte mineral district is located in the Central Srednogorie zone, 60–90 km east of Sofia, and has supplied about 95% of the Bulgarian Cu and Au production (465 Mt ore in past production, Strashimirov et al. 2002), from porphyry–Cu and Au–Cu epithermal deposits (Mutafchiev and Petrunov 1996, unpublished report). These ore deposits are aligned along a NNW trend, which is oblique to the EW trend of the Srednogorie belt (Fig. 1b).

Metamorphic basement rocks of the Panagyurishte district consist predominantly of migmatite, amphibolite, and gneiss, interpreted as Precambrian, and defined as Pirdop Group by Dabovski (1988), Srednogorie-type metamorphic rocks by Cheshitev et al. (1995) and Pre-Rhodopean Supergroup by Katskov and Iliev (1993). In contrast, Ivanov (1989) named them the Balkanide-type metamorphic complex and inferred a Paleozoic age, an interpretation supported by U–Pb zircon ages (Arnaudov et al. 1989; Peytcheva and von Quadt 2004). Low-grade metamorphic basement rocks of the Berkovitsa Group in the northern part of the Panagyurishte district consist of phyllite, chlorite schist, and diabase, interpreted as Late Precambrian to Cambrian by Haydoutov et al. (1979) and Haydoutov (2001). Basement intrusions consist of Paleozoic gabbrodiorites, quartz diorites, tonalites, and granodiorites to granites (Dabovski et al. 1972; Kamenov et al. 2002; Peytcheva and von Quadt 2003, 2004; Carrigan et al. 2005). All these units underwent ductile deformation and associated low-grade metamorphism at ~100 Ma (Velichkova et al. 2004) and are unconformably covered by Late Carboniferous to Jurassic clastic and carbonate sedimentary rocks and Turonian conglomerate and sandstone, containing metamorphic rock fragments and coal-bearing interbeds (Fig. 1b; Foose and Manheim 1975; Aiello et al. 1977; Moev and Antonov 1978; Cheshitev et al. 1995; Stoykov and Pavlishina 2003). These sedimentary rocks are also overlain by the Turonian to Maastrichtian Srednogorie volcano-sedimentary basin, which consists of magmatic rocks and intra-arc sandstones, conglomerates, subordinate pelagic marlstones, shales, and turbidites (Fig. 1b; Aiello et al. 1977; Moev and Antonov 1978; Popov 2001; Stoykov and Pavlishina 2003).

The Late Cretaceous magmatic rocks are calc-alkaline to high-K calc-alkaline with a local transition to subalkaline, and their geochemical composition is consistent with magmatism related to an active continental volcanic arc (Popov and Popov 1997; Stoykov et al. 2002, 2003; Kamenov et al. 2003a,b; von Quadt et al. 2005a). Andesitic and subvolcanic to effusive rocks predominate in the north, whereas dacitic and holocrystalline intrusive rocks are more abundant in the southern part (Fig. 1b; Boccaletti et al. 1978; Stanisheva-Vassileva 1980). Small, subvolcanic dacite, quartz monzodiorite, and granodiorite intrusions (mostly <1 km^2 in size) are comagmatic with the Late Cretaceous volcanic rocks. Larger, syntectonic, Late Cretaceous granodioritic–granitic intrusions are restricted to the southernmost Panagyurishte district along the Iskar–Yavoritsa Shear Zone (Fig. 1b; Ivanov et al. 2001; Peytcheva et al. 2001; Georgiev and Ivanov 2003; Peytcheva and von Quadt 2003).

Local geological and metallogenic setting

The Chelopech deposit is located about 6 km southeast of the Elatsite porphyry–Cu deposit (Fig. 2a). The Late Cretaceous volcanic and volcano-sedimentary complex, which hosts the Chelopech epithermal deposit, transgressively overlie the Precambrian and Paleozoic metamorphic basement rocks (Figs. 2a–c, 3; Popov et al. 2000). The Late Cretaceous sedimentary succession starts with coal-bearing sandstone and conglomerate, which is crosscut by subvolcanic bodies and overlain by the Chelopech Formation, which in turn is composed of argillaceous limestone, calcarenite, and sandstone interlayered with volcanic rocks (Moev and Antonov 1978). Paleontological dating by Stoykov and Pavlishina (2003) yields a Turonian age for

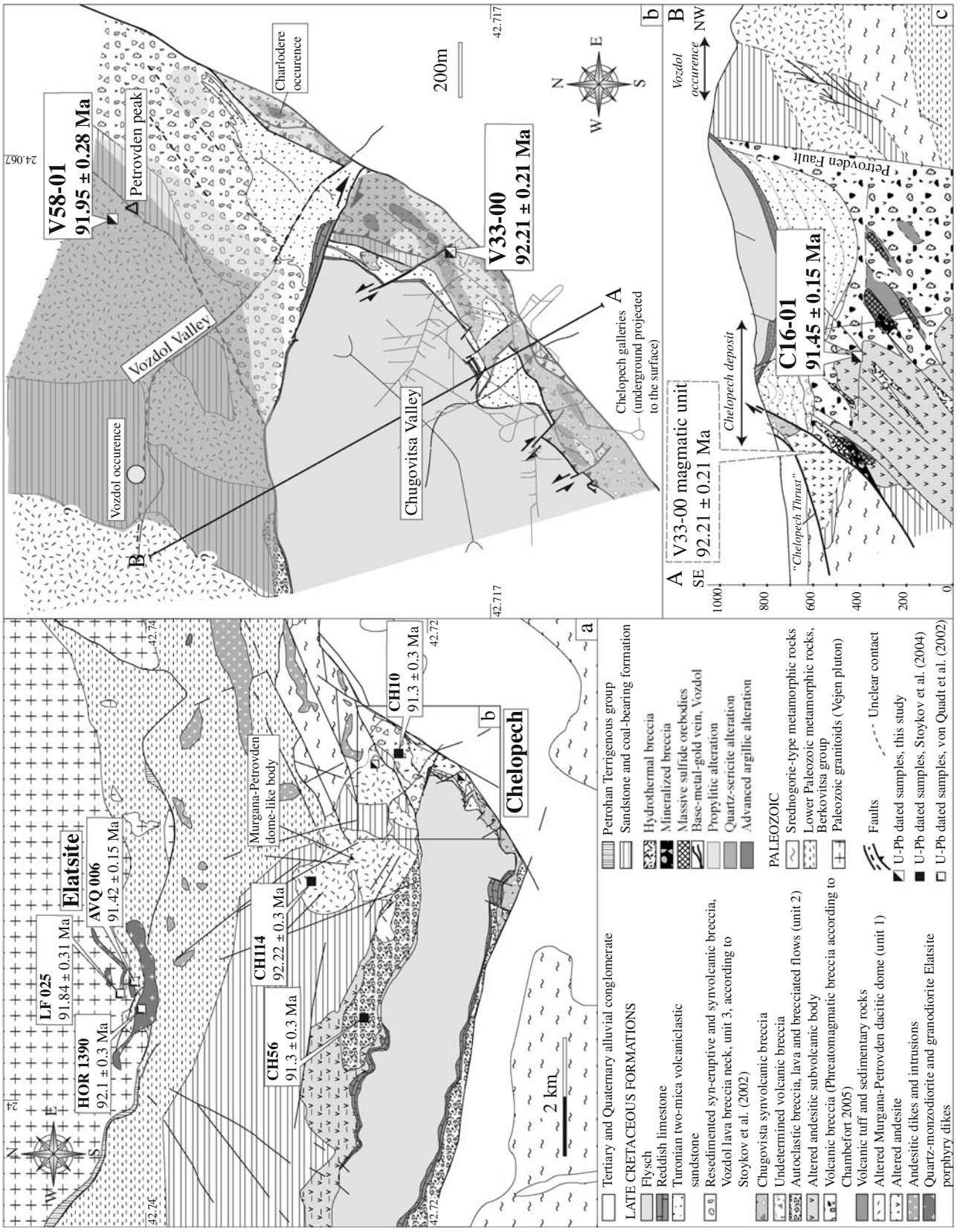

Fig. 2 **a** Geological map of the northern part of the Panagyurishte ore district, modified from Popov and Popov (2000) and Stoykov et al. (2004). **b** Surface geological map of the Chelopech epithermal deposit area (Georgieva 2003, personal communication; Chambefort 2005). **c** Cross-section of the Chelopech epithermal deposit (Chambefort 2005)

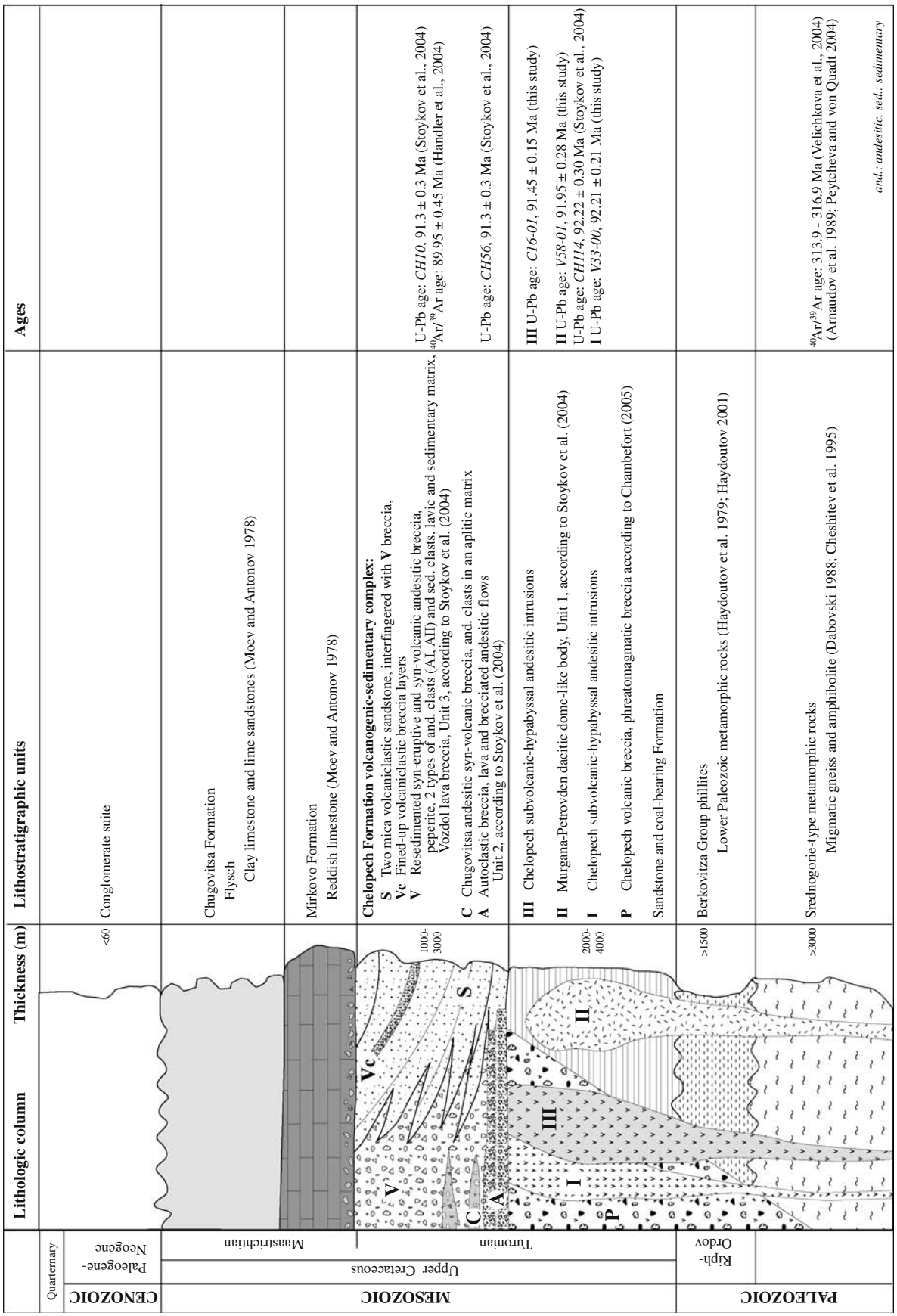

Fig. 3 Stratigraphic column of the Chelopech district (modified after Popov and Popov 2000)

both the basal sandstone and conglomerate and the uppermost part of the Chelopech Formation (i.e. the Turonian two-mica volcaniclastic sandstone in Figs. 2b,c, 3). The Santonian–Campanian limestone and marlstone of the Mirkovo Formation, and the calcarenite and mudstone flysch of the Chugovitsa Formation overlie the Chelopech Formation (Moev and Antonov 1978).

On the basis of K–Ar dating by Chipchakova and Lilov (1976) and petrological studies, Popov and Kovachev (1996) and Popov and Popov (1997, 2000) distinguished four independent Late Cretaceous magmatic stages in the Chelopech area. The oldest unit comprises the dacitic dome-like bodies of Murgana and Petrovden to the north of Chelopech (Fig. 2a). The second stage is a sequence of andesitic agglomerate, rare ash tuff, intercalated with andesitic lava flows and lava sheets. According to Popov and Kovachev (1996), rocks of this stage were intruded by several successive necks and late subvolcanic andesitic intrusions at Chelopech. Epithermal ore formation overprints the latter. The latest magmatic event described by Popov and Kovachev (1996), Popov and Popov (2000), and Popov et al. (2000) is the emplacement of a volcanic breccia, which crops out along the Vozdol Valley, and is interpreted as a volcanic neck (see Vozdol lava breccia neck, Unit 3 in Fig. 2b).

Recently, Stoykov et al. (2002, 2004) proposed three different phases for the Chelopech volcanism linked to a Late Cretaceous island arc setting:

1. A dome-like body is developed in the Turonian sedimentary rocks and is well exposed in the Murgana area (sample area CH114, Unit 1, in Fig. 2a). It has an andesitic to trachydacitic composition with a porphyritic texture displaying a microlitic groundmass (Stoykov et al. 2002, 2004).

2. Lava and agglomerate flows have been described in the northern part of the Chelopech area (sample area CH56, Unit 2, in Fig. 2a). The composition of lava flows is chiefly latitic, has an amphibole- and plagioclase-bearing porphyritic texture, and accessory biotite and titanite. The groundmass is microlitic, with plagioclase microlites. The presence of magmatic xenoliths, with almost the same mineralogy, is interpreted by Stoykov et al. (2002) as evidence of mingling.

3. Lava breccia is present in the eastern part of the Vozdol Valley to the northeast part of the Petrovden area (Fig. 2b; sample area CH10, Unit 3, in Fig. 2a). Popov et al. (2000) and Stoykov et al. (2002, 2004) interpret this breccia as the youngest volcanic event in the Chelopech magmatic zone, and they named this rock "the Vozdol neck monovolcano". The Vozdol "neck" consists of clast-supported lava-breccia. The Vozdol breccia clasts are andesitic and latitic in composition and have petrographic characteristics similar to lava and agglomerate flows, in which, phenocrysts are less abundant (Stoykov et al. 2002, 2004).

Our study shows that magmatic rocks represent approximately 40% of the surface exposure in the immediate vicinity of the Chelopech mine (Fig. 2b). Directly above the deposit, only strongly altered magmatic rocks are present, which are also recognized in the Petrovden area. Turonian two-mica sandstone and Maastrichtian limestone and flysch are not altered. Altered dacite in the Petrovden area (Fig. 2b) probably belongs to the Murgana dome-like body defined by Stoykov et al. (2002).

The Vozdol volcanic breccia is overlain by and interfingered with the two-mica sandstone of the Chelopech Formation (Figs. 2b and 3; Chambefort 2005). This observation documents a synchronous deposition of the breccia with the base of the sandstone unit during the Turonian (Stoykov and Pavlishina 2003). This volcanic breccia contains andesitic and sedimentary clasts (Fig. 2b) inside an altered aplitic lava and/or sedimentary matrix. The sedimentary clasts are composed of unaltered, rounded, fine-grained volcaniclastic sandstone typical of the two-mica sandstone of the Chelopech Formation. Two types of magmatic clasts are recognized and referred to as AI and AII. The two types of magmatic clasts are differentiated based on texture, mineralogy, and geochemistry (Chambefort 2005). The proportion of the type AII clast decreases from the southwest in the Vozdol Valley (Fig. 2b) to the northeast, but both clast types are present in the outcrops. This volcanic breccia unit includes different textural facies. Andesitic hyaloclastite zones are characterized by an intensively altered glass matrix, mostly oxidized, with a distinct jigsaw-fit texture. Sedimentary clasts can be incorporated into the altered aplitic lava matrix, which is characteristic of peperitic breccia formation (Chambefort et al. 2003; Chambefort 2005). Some pillow lava clasts have been identified based on concentric and radial joints. The presence of magmatic clasts inside a sedimentary matrix with sharp and unquenched contacts suggests that some parts of this volcanic breccia have been resedimented during late sedimentary processes or at the periphery of the volcanic system during syn-volcanic breccia formation. Therefore, this breccia is renamed as a resedimented and syn-volcanic andesitic breccia (Figs. 2, 3).

The Chelopech high-sulfidation deposit belongs to the northern part of the Panagyurishte mineral district (Fig. 1), which includes the Vozdol base–metal–quartz–carbonate veins (Fig. 2b, Mutafchiev and Petrunov 1996, unpublished report; Popov et al. 2000), the Karlievo porphyry–Cu occurrence (Fig. 1), and the Elatsite porphyry–Cu deposit, located 6 km to the north of Chelopech (Fig. 2a). Popov et al. (2001) recognize a regional high geomagnetic anomaly beneath this ore deposit cluster, which they interpret as a

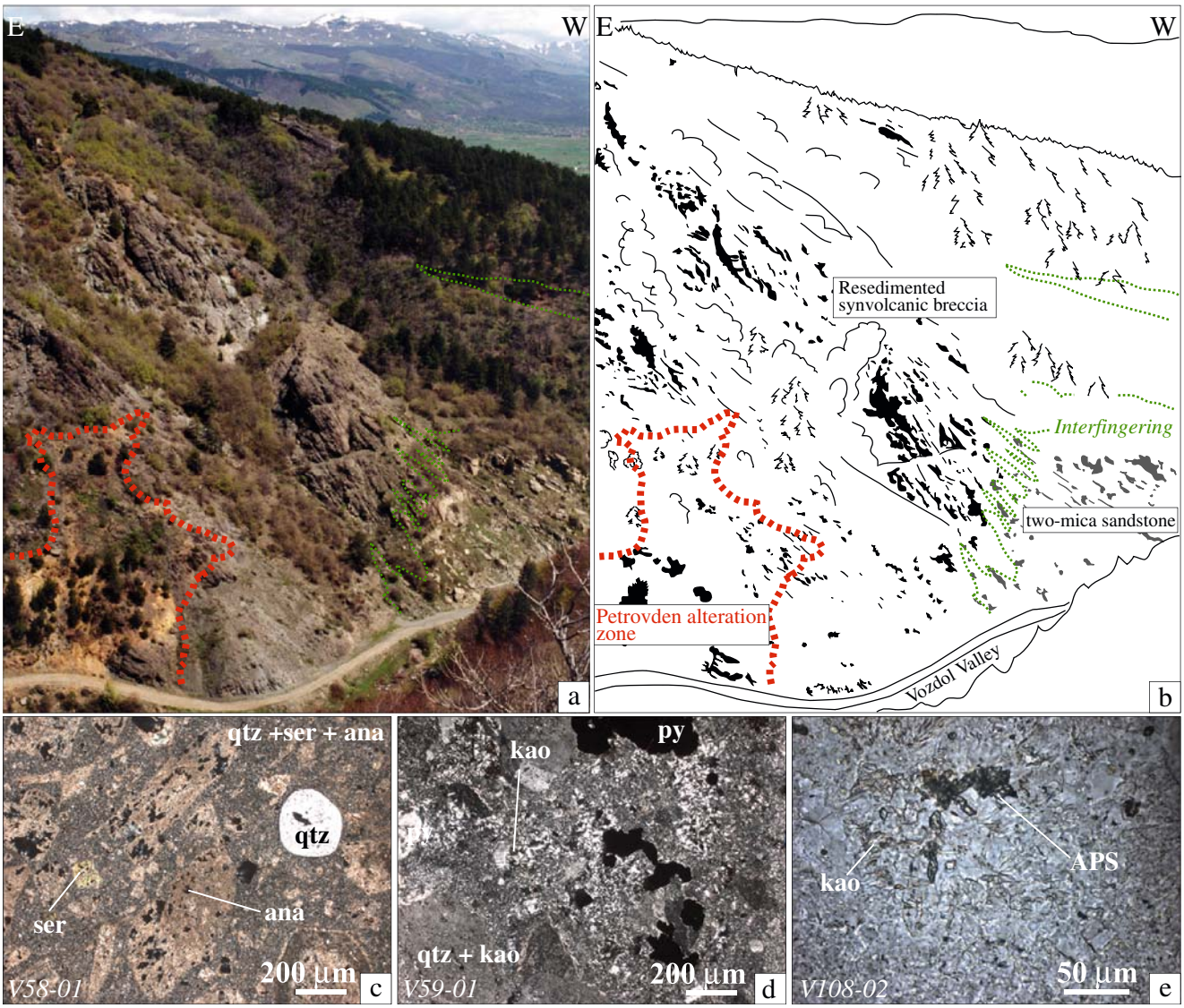

Fig. 4 Overview of the Petrovden alteration zone, affecting the resedimented and synvolcanic breccia of Vozdol. **a, b** Outcrop of the resedimented, synvolcanic Vozdol breccia, interfingering with the two-mica volcaniclastic sandstone. The Vozdol breccia has been overprinted by the Petrovden alteration zone in the eastern part of the outcrop. **c** Quartz–sericite altered sample of the Petrovden dacitic dome-like body, with preserved porphyritic texture, including plagioclase and amphibole ghosts. **d** Argillic altered sample of the Petrovden dacitic dome-like body. **e** Argillic alteration zone of the Petrovden alteration area, alumino–phosphate–sulfate minerals. (*ana* anatase, *APS* alumino–phosphate–sulfate minerals, *kao* kaolinite, *py* pyrite, *qtz* quartz, *ser* sericite)

shallow large magmatic chamber. Next to Chelopech, the Elatsite porphyry–Cu deposit is the major producing mine in the northern Panagyurishte district with Cu and Au grades of 0.44% and 0.2 g/t, respectively (Fig. 2a). Ore minerals include chalcopyrite and pyrite and subsidiary molybdenite, gold, and platinum-group minerals (Kalaidjiev et al. 1984; Petrunov and Dragov 1993; Strashimirov et al. 2002; von Quadt et al. 2002, 2005b; Tarkian et al. 2003). The Elatsite porphyry–Cu deposit is associated with Late Cretaceous subvolcanic bodies and porphyry dikes (Kalaidjiev et al. 1984; von Quadt et al. 2002), which intrude rocks of the Berkovitsa group (Haydoutov 1987) and granodiorites of the Vejen pluton (314 Ma, Kamenov et al. 2002, 2003a). The Late Cretaceous andesitic, granodioritic, and monzodioritic dikes at Elatsite and around the deposit occur in swarms (Fig. 2a). One of the largest dikes, the so-called big dike, is 4 km long and 100–450 m wide, dips 40–45° to the south, and has been interpreted as a hypabyssal branch of a larger intrusive body at depth (von Quadt et al. 2002). No volcanic rocks are exposed in the vicinity of the Elatsite deposit; the closest outcrop is in the Chelopech area (Fig. 2a). Lower Paleozoic phyllites of the Berkovitsa group (Haydoutov et al. 1979), a

Turonian sandstone and coal-bearing formation, and epiclastic rocks are exposed between the Elatsite and Chelopech deposits (Fig. 2a; Stoykov et al. 2004).

The Chelopech epithermal high-sulfidation Au–Cu deposit and relative timing of ore formation

The Chelopech deposit is hosted by a hypabyssal magmatic body of andesitic composition, altered volcanic breccia, (recently characterized as a breccia of phreatomagmatic origin) (Fig. 3, Chambefort 2005), and subsidiary altered volcanic tuff containing accretionary lapilli and pumices interbedded with sedimentary rocks with oolitic, biodetrital, and sandstone layers (Jacquat 2003; Chambefort 2005; Moritz et al. 2005). These rock units, which are only exposed within the underground mine, belong to the Chelopech Formation. Neither hydrothermal alteration nor any high-sulfidation mineralization affects the overlying Mirkovo and Chugovitsa Formations. Therefore, the relative age of the Chelopech deposit is Turonian based on pollen dating by Stoykov and Pavlishina (2003). The Chelopech deposit displays a typical epithermal high-sulfidation alteration, from an innermost advanced argillic alteration zone with vuggy silica, through quartz–sericite alteration to distal propylitic alteration (Georgieva et al. 2002). The mineralization includes three successive ore-forming stages: (1) an early Fe–S pyrite–marcasite stage, with disseminated to massive pyrite replacement bodies, the latter being particularly well developed along volcanic tuff and sedimentary rock layers, (2) an intermediate Au-bearing Cu–As–S stage, which constitutes the economic ore stage, characterized by the presence of enargite, luzonite, tennantite, bornite, and native gold, and (3) a late-stage, uneconomic base–metal vein stage with sphalerite and galena (Petrunov 1994, 1995; Jacquat 2003; Moritz et al. 2004, 2005; Chambefort 2005). The Chelopech Mine produces approximately 130,000 oz gold/year and 21,700 t copper/year of ore and contains 22 Mt measured and indicated reserves, at 3.6 g/t gold and 1.4% Cu (Dundee Precious Metals Inc. data; http://www.dundeeprecious.com/). Hydrothermal alteration and ore formation have been both lithologically and structurally controlled (Chambefort 2005; Chambefort and Moritz 2006). The Late Cretaceous ore-controlling faults have been reactivated during Tertiary Alpine orogenic events, displacing older rock units over the ore bodies along the Chelopech Thrust (Fig. 2c; Chambefort and Moritz 2006). The overthrust of older rock units on top of the Chelopech deposit and post-ore sedimentation of the Mirkovo and Chugovitsa Formations provided a favorable environment for the exceptional preservation of this Late Cretaceous epithermal deposit.

Popov and Kovachev (1996) and Popov et al. (2000) mention the occurrence of mineralized clasts in the volcanic breccia of the Vozdol Valley (Fig. 2b). They thus interpreted

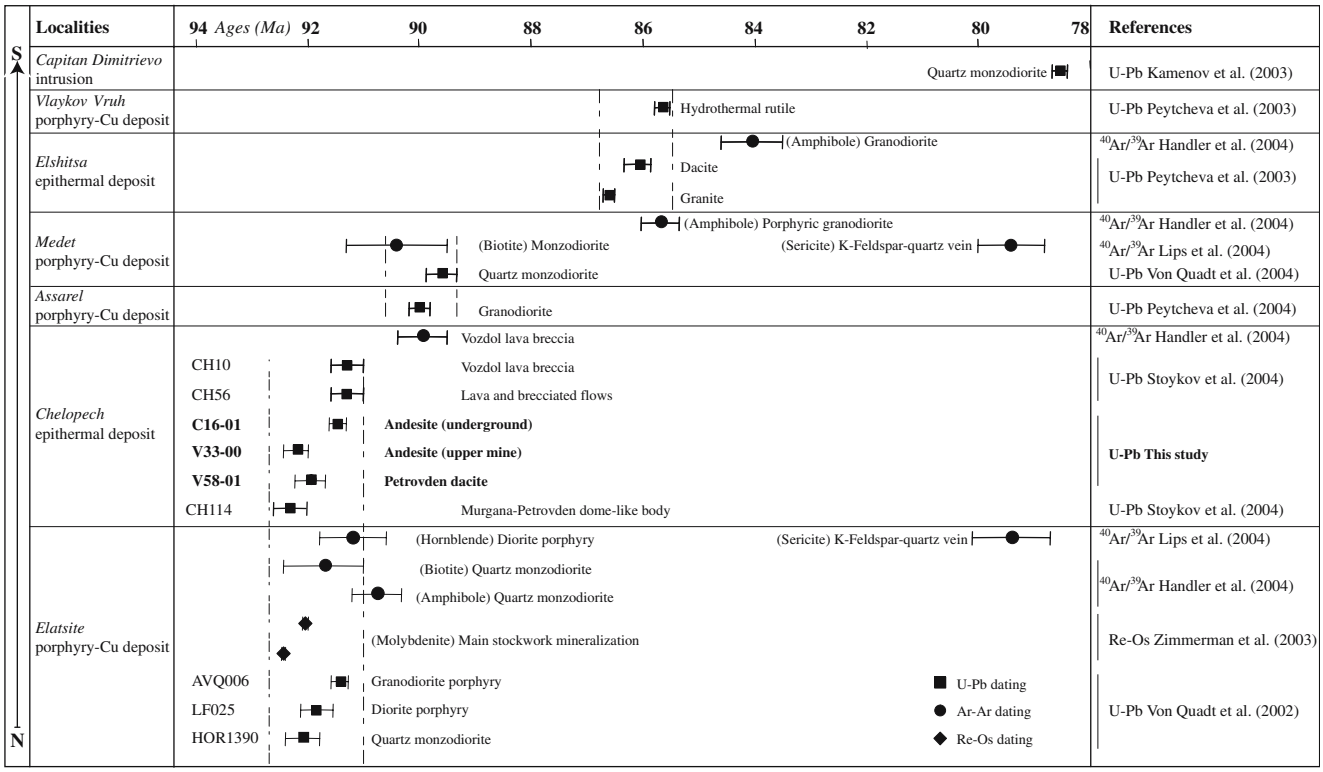

Fig. 5 Timing of magmatism and ore formation in the Panagyurishte mineral district

this neck as a post-ore magmatic event crosscutting the ore bodies at depth. By contrast, Chambefort (2005) interpreted it as a resedimented and syn-volcanic breccia, which formed during the emplacement of lava into unconsolidated sediments in a shallow basin as documented by the interfingering of the breccia and the two-mica sandstone (Figs. 3 and 4a,b). However, both interpretations agree that the Vozdol breccia unit constitutes the latest magmatic event in the Chelopech vicinity.

The altered volcanic rock clasts in the Vozdol breccia unit contain a hydrothermal alteration assemblage of fine-grained quartz, dickite, kaolinite, barite, pyrite, anatase, and alumino–phosphate–sulfate minerals (Georgieva et al. 2004). Georgieva et al. (2004) state that such alteration is typical of the upper part of the Chelopech deposit and, therefore, conclude that the presence of these altered clasts in the Vozdol breccia sets a minimum age limit for ore formation at Chelopech. However, there are other alteration zones in the area, including the fault-controlled quartz–sericite (Fig. 4c) and argillic alteration (Fig. 4d,e) in the Petrovden area (Figs. 2b, 4a) with a hydrothermal alteration assemblage composed of quartz, kaolinite, dickite, pyrite (Fig. 4d), anatase, and alumino–phosphate–sulfate minerals (Fig. 4e), which have affected the Petrovden dacitic dome, the Vozdol breccia unit, and the Turonian sandstone and coal-bearing formation (Popov and Kovachev 1996; Jelev et al. 2003). Thus, a single origin cannot be unambiguously attributed to the altered clasts in the Vozdol breccia, making the age interpretation uncertain. Moreover, no field relationships exist to constrain the relative timing of the hydrothermal alterations at Petrovden (Fig. 4a,b) and Chelopech.

Previous dating in the Panagyurishte area

Early, potassium–argon age determination of whole rocks and mineral separates from the Panagyurishte mineral district suggested four magmatic stages ranging between 91 and 65 Ma (Chipchakova and Lilov 1976; Lilov and Chipchakova 1999). More recent radioisotopic investigations include $^{40}Ar/^{39}Ar$, U–Pb, and Re–Os dating, which are better capable of unraveling the polyphase evolution of magmatism, deformation, and ore formation of the Panagyurishte district. Pre-Cretaceous metamorphic and magmatic events of the Panagyurishte district are not considered here (see Zagorchev and Moorbath 1987; Arnaudov et al. 1989; Kamenov et al. 2002; Peytcheva and von Quadt 2004; Velichkova et al. 2004; Carrigan et al. 2005); only dating of Late Cretaceous events is summarized below.

Available U–Pb zircon data from the Panagyurishte mineral district show a 14-My-long protracted Late Cretaceous magmatic and hydrothermal evolution (Fig. 5), with magmatic and ore-forming events becoming progressively younger from north to south across the EW-trending Srednogorie zone (von Quadt et al. 2005a). In the northern Panagyurishte district, at the Elatsite porphyry–Cu deposit (Fig. 1), magmatism and ore formation started at 92.1±0.30 (von Quadt et al. 2002), and porphyry–Cu ore formation was completed within 900,000 years (von Quadt et al. 2005a). Re–Os ages of 92.43±0.04 to 92.03±0.05 Ma (Zimmerman et al. 2003), suggesting a minimum absolute life span of 400,000±90,000 years for the stockwork mineralization, are in agreement with U–Pb data. Intrusive activity in the central part of the Panagyurishte district at Medet and Assarel (Figs. 1 and 5) is slightly younger, with U–Pb zircon ages between 90.06±0.22 and 89.61±0.26 Ma (von Quadt and Peytcheva 2004; von Quadt et al. 2005a), and was followed by magmatism at Elshitsa and porphyry–Cu ore formation at Vlaykov Vruh (Figs. 1 and 5) dated at 86.62±0.11 to 86.11±0.23 Ma and 85.65±0.15 Ma, respectively (Peytcheva et al. 2003). The youngest magmatic event dated by U–Pb in the southern Panagyurishte district is the emplacement of the Capitan Dimitrievo pluton at 78.54±0.13 Ma (Kamenov et al. 2003a,b). The progressive southward migration of magmatism and ore formation is explained as a consequence of slab rollback (Kamenov et al. 2003a,b, 2004; von Quadt et al. 2003) or southward retreat of the subducting slab (Handler et al. 2004; von Quadt et al. 2005a).

$^{40}Ar/^{39}Ar$ dating by Velichkova et al. (2004) indicates that low-grade Alpine metamorphism occurred at about 106–100 Ma and, therefore, predates Late Cretaceous magmatic activity within the Panagyurishte district. Incremental heating experiments of biotite and amphibole from Late Cretaceous magmatic rocks of the Panagyurishte district by Handler et al. (2004) yield $^{40}Ar/^{39}Ar$ plateau ages between 91.72±0.70 and 80.21±0.45 Ma that agree with the north-to-south younging, indicated by the U–Pb zircon ages (Fig. 5). However, the $^{40}Ar/^{39}Ar$ ages are systematically and, in some cases, significantly younger in a given locality than the U–Pb zircon ages (von Quadt et al. 2005a). Therefore, the $^{40}Ar/^{39}Ar$ ages most likely reflect post-magmatic and post-ore formation cooling ages. Most $^{40}Ar/^{39}Ar$ age spectra reveal a weak Eocene to Early Oligocene thermal overprint at about 40–32 Ma (Handler et al. 2004). Lips et al. (2004) also report $^{40}Ar/^{39}Ar$ ages for magmatic hornblende and biotite and hydrothermal white mica from the Elatsite and Medet porphyry–Cu deposits (Figs. 1 and 5). Magmatic hornblende from Elatsite and biotite from Medet yielded ages of 91.2±0.6 and 90.4±0.9 Ma, which overlap within uncertainty with U–Pb ages obtained by von Quadt et al. (2002, 2005a; Fig. 5). White micas from alteration assemblages from both deposits yielded younger $^{40}Ar/^{39}Ar$ ages between 79.0±0.8 and 79.9±0.7 Ma. At Elatsite, for example, these white mica ages have no geological connection with ore-forming

Table 1 Representative geochemical analyses of fresh and altered magmatic rocks of the Chelopech deposit area

Units		Vozdol syn-eruptive andesitic breccia		Altered andesite underground		Altered andesite surface		Altered dacite (Petrovden)		Volcanic tuff (mine)	
Samples	2σ	V1-00	V7-00	C16-01	C75-01	V33-00	V62-01	V59-01	V58-00	C54-01	C56-01
%											
SiO_2	0.3	59.83	62.99	63.43	75.11	70.29	60.90	63.72	68.92	82.67	74.80
Al_2O_3	0.2	18.91	17.60	19.24	10.92	17.13	18.45	17.80	15.66	7.95	14.77
Fe_2O_3	0.1	4.40	4.49	4.14	4.76	0.90	5.29	3.45	4.27	2.56	1.67
MnO	0.02	0.07	0.09	0.02	0.01	0.00	0.10	0.08	0.02	0.01	0.00
MgO	0.15	1.20	1.46	0.64	0.49	0.27	0.44	2.35	0.72	0.45	0.01
CaO	0.15	4.40	3.00	0.42	0.22	0.16	2.72	0.20	0.03	0.12	0.03
Na_2O	0.15	6.27	5.84	0.35	0.22	0.21	4.08	2.49	0.10	0.19	0.06
K_2O	0.06	2.01	2.07	4.30	2.74	7.26	5.40	3.55	4.59	1.94	0.07
TiO_2	0.03	0.55	0.57	0.63	0.39	0.59	0.59	0.49	0.55	0.26	0.51
P_2O_5	0.02	0.24	0.25	0.26	0.14	0.02	0.26	0.18	0.04	0.10	0.20
LOI 1,100°C		1.66	1.22	6.21	5.26	2.71	2.10	5.85	5.24	3.23	7.40
Total		99.54	99.58	99.64	100.26	99.54	100.33	100.16	100.14	99.48	99.52
(ppm)											
V	8	133	142	173	91	131	149	126	84	67	109
Cr	8	17	13	18		13	10	15			
Ga	3	15	17	21	17	18	19	21	21	11	27
Co	3	54	34	10	30	23	24	14	42	20	40
Sc	2	11	10	6	7	3	9	7	7	5	6
Y	4	26	22	36	29	8	20	17	21	17	4
Nb	5	8	8	5	6	7	8	8	9	4	7
Zr	30	101	89	145	91	155	130	135	169	47	129
Sr	9	906	948	41	182	37	676	131	10	76	1,900
Ba	40	583	808	90	2,427	317	817	483	509	220	5,718
Rb	7	34	38	187	115	307	241	144	186	95	1
Pb	6	10	16	47	264	7	12	83	77	42	157
Th	7	3	6	9	6	8	9	10	8	4	6
U	1	2	2	4	2	5	2	2	2	1	2
Cu	9	10	26	38	72	6	18	31	12	205	107
Zn	11	45	57	29	110	20	63	199	31	120	19
As	1.5	11	12	16	110	12	7	3	5	21	9
Ag	0.5	–	–	0	8	–	–	–	0	–	1
Au (ppb)	35	–	–	132	378	–	–	3	19	20	8
S%	1.7	0	0	3	5	0	0	3	4	3	2
(ppm)	(10%)										
La		28.8	26.6	25.9	22.0	14.0	45.2	28.1	40.4	46.2	37.5
Ce		58.5	55.4	55.0	38.4	32.1	82.9	53.3	77.0	70.5	80.2
Pr		6.4	6.2	6.2	3.8	3.4	8.8	5.4	8.5	6.9	8.3
Nd		26.1	24.6	26.1	13.9	11.7	33.5	19.6	30.9	24.6	28.6
Sm		6.8	6.0	5.1	3.2	2.8	6.1	3.4	5.3	3.8	3.5
Eu		1.5	1.4	1.2	1.3	0.6	1.7	1.0	1.1	1.0	1.1
Gd		4.4	4.1	4.0	4.4	1.7	4.8	2.7	4.3	3.3	1.7
Dy		4.0	3.9	4.5	5.1	2.3	3.5	2.2	3.5	3.0	0.6
Ho		0.8	0.7	1.0	1.0	0.4	0.7	0.4	0.7	0.6	0.1
Er		2.1	2.0	2.5	2.7	1.2	2.0	1.4	2.1	1.8	0.6
Tm		0.3	0.3	0.4	0.4	0.2	0.3	0.2	0.3	0.3	0.1
Yb		1.9	1.8	2.3	2.3	1.2	2.0	1.5	2.2	1.6	0.8
Lu		0.3	0.3	0.3	0.3	0.2	0.3	0.2	0.3	0.2	0.1

Major and trace elements: X-ray fluorescence, University of Lausanne; REE: inductively coupled plasma atomic emission spectrometry, University of Geneva (Voldet 1993)

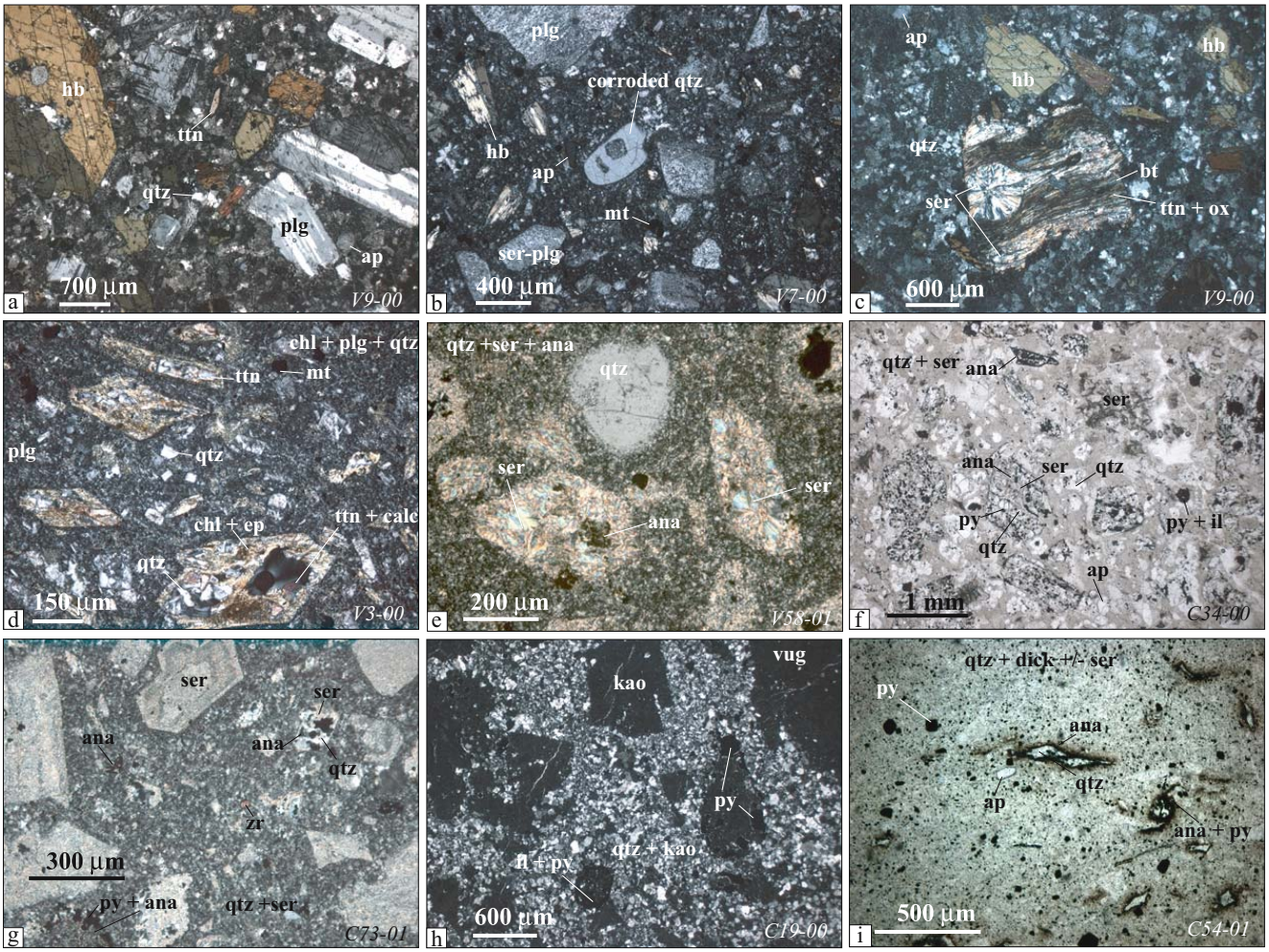

Fig. 6 Different magmatic textures and alteration assemblages of the magmatic rocks from the Chelopech area. **a** Porphyritic texture of the syn-eruptive Vozdol breccia clast, **b** Corroded quartz phenocryst in a porphyritic clast of the Vozdol breccia, **c** Typical biotite alteration with titanite, sericite, and oxide in so-called fresh samples, **d** Propylitic altered sample with relict porphyric texture, **e** Quartz–sericitic altered sample of the Petrovden area, with a resorbed quartz phenocryst, **f** Quartz–sericite altered sample of underground subvolcanic rocks at Chelopech with preserved porphyric texture, including amphibole ghosts, block 18 level 405, **g** Quartz–sericitic altered mine sample with porphyric texture showing totally sericitized plagioclase major phenocrysts, **h** Mine sample with advanced argillic alteration, with preserved porphyric texture and plagioclase phenocrysts totally replaced by clay minerals. Note the presence of vuggy silica, block 151 level 405. **i** Preserved volcanic tuff "pumice", block 151 western gallery level 405. (*ana* anatase, *ap* apatite, *APS* alumino–phosphate–sulfate minerals, *bt* biotite, *calc* calcite, *chl* chlorite, *dick* dickite, *ep* epidote, *hb* hornblende, *il* ilmenite, *kao* kaolinite, *mt* magnetite, *ox* oxide, *plg* plagioclase, *py* pyrite, *qtz* quartz, *ser* sericite, *ttn* titanite, *vug* vuggy silica)

processes at about 92 Ma as evidenced by the U–Pb zircon age constraints provided by von Quadt et al. (2002; Fig. 5). Therefore, as suggested by Lips et al. (2004), these young ages most likely reveal argon loss or thermal resetting.

Within the Chelopech area, the oldest dated rock unit is the dacitic dome-like body at Murgana, approximately 3.5 km to the northwest of the Chelopech mine (Stoykov et al. 2004; sample CH 114 in Fig. 2a), which yielded a U–Pb zircon age of 92.22±0.30 Ma. An U–Pb age of 91.3± 0.30 Ma was obtained for both an andesite clast of the Vozdol breccia immediately to the northeast of the mine and for a brecciated andesite lava flow between Murgana and the Chelopech mine (Stoykov et al. 2004; samples CH 56, CH10 in Fig. 2a). They interpret the former as the youngest magmatic event, and the age is slightly at variance with a $^{40}Ar/^{39}Ar$ age of biotite from the same Vozdol breccia of 89.95±0.45 Ma, interpreted by Handler et al. (2004) as a magmatic event.

Analytical techniques

Major and trace elements were analyzed by X-ray fluorescence at the University of Lausanne, Switzerland, using a Philips PW 1400. The relative 2σ precision of major and trace element analyses is listed in Table 1. Loss on ignition (LOI) was determined by igniting a weighed sample at 1,050°C. Rare earth elements (REE) were analyzed by ICP-

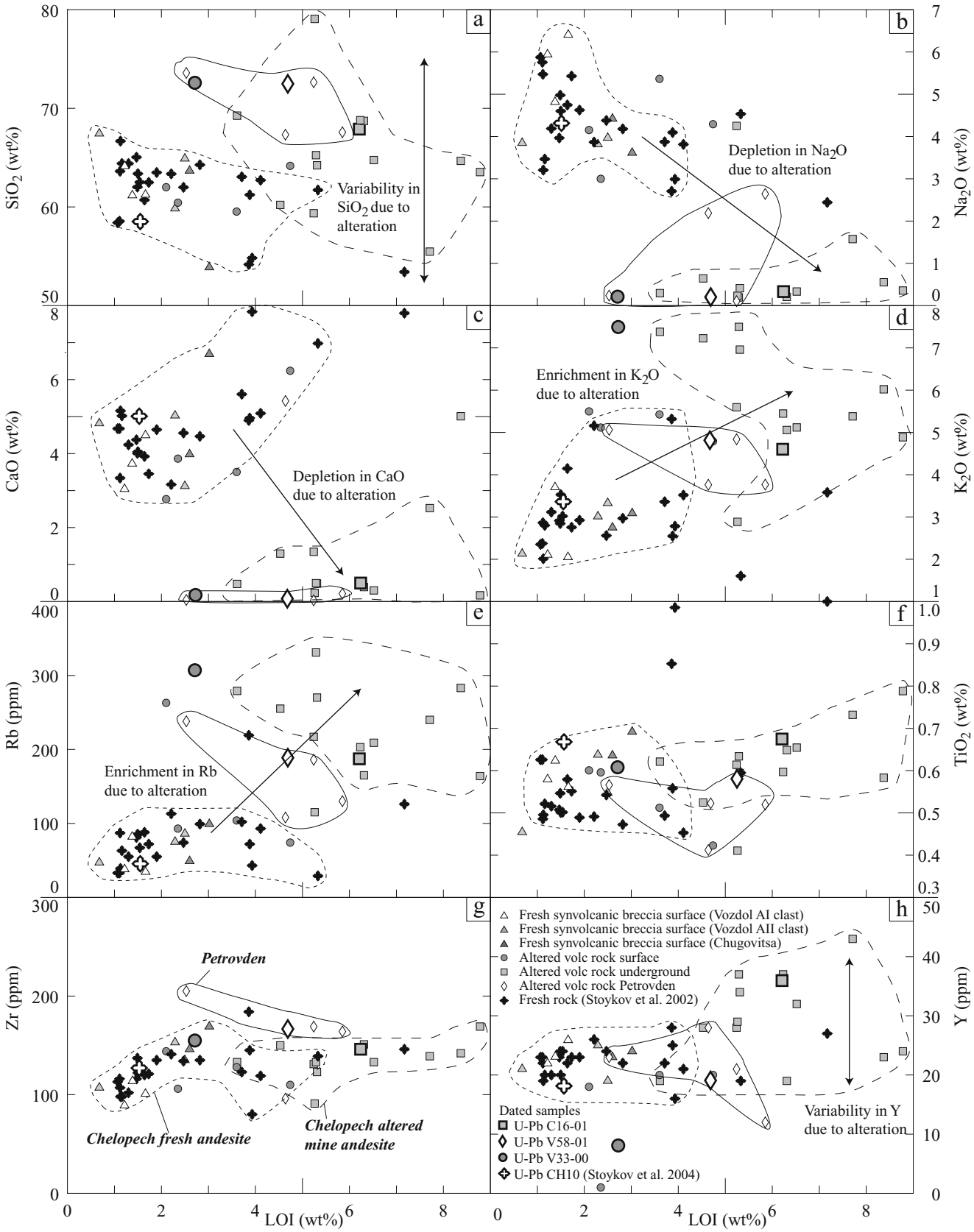

Fig. 7 Major and trace elements vs LOI. LOI is considered as an alteration index

AES at the University of Geneva following the procedure of Voldet (1993). The 2σ precision is 5–10%.

Cathodoluminescence images of zircons were photographed on a CamScan MV2300 SEM at the University of Lausanne, operating at 15 kV.

High-precision conventional U–Pb zircon analyses were performed on single zircon grains at the ETH Zurich, Switzerland. Selected zircons were air-abraded to remove marginal zones with lead-loss, washed in warm 4 N nitric acid and rinsed several times with distilled water and acetone in an ultrasound bath. Dissolution and chemical extraction of U and Pb was performed following Krogh (1973), using a ^{205}Pb–^{235}U spike. Both Pb and U were loaded with silica gel and phosphoric acid on single Re

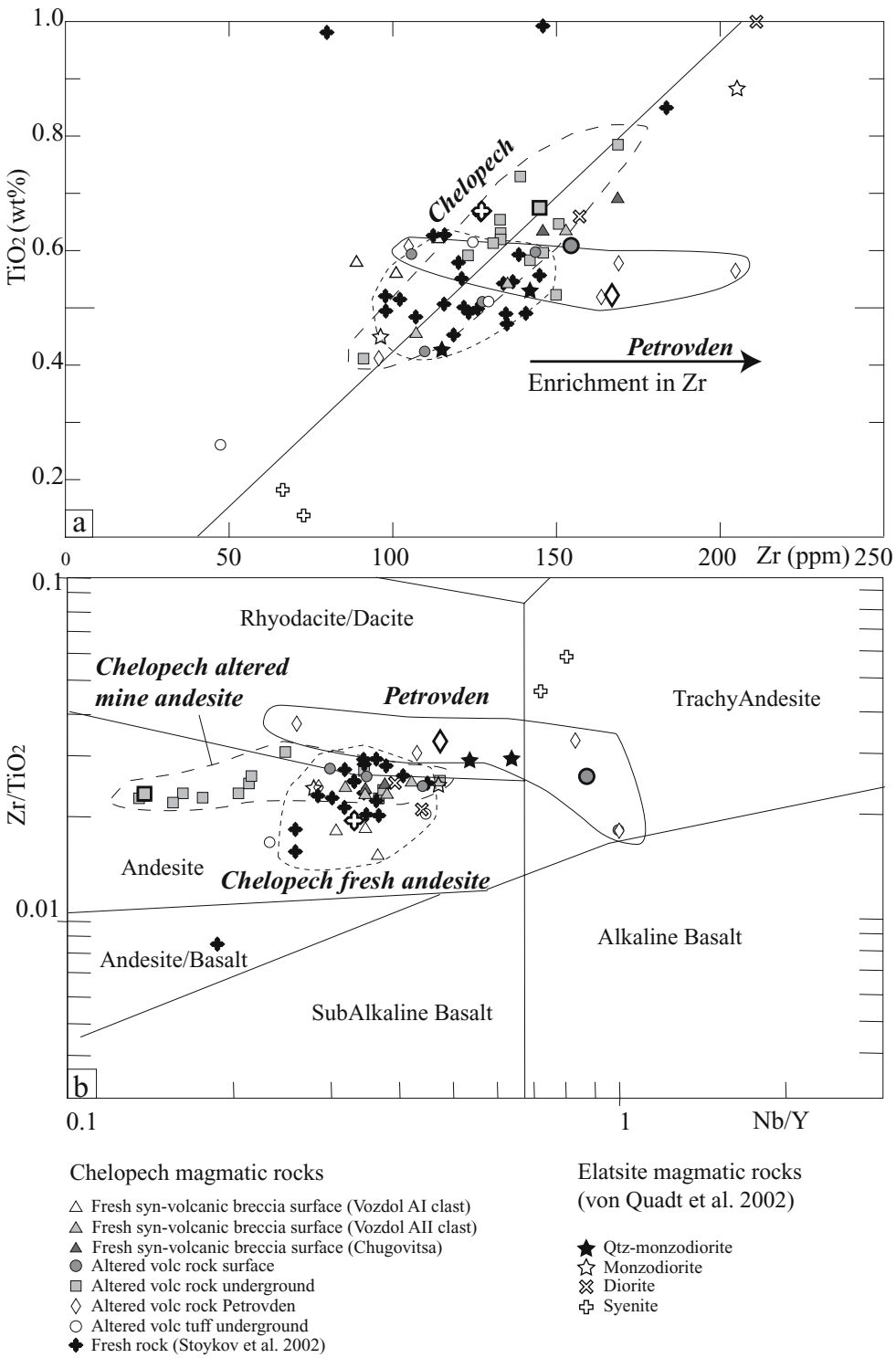

Fig. 8 **a** Zr (ppm) vs TiO_2 (wt %) plot of magmatic rocks from the Chelopech, Petrovden, and Elatsite area. **b** Classification of the magmatic rocks from the Chelopech area according to Winchester and Floyd (1977), including Elatsite analyses from von Quadt et al. (2002)

filaments and measured on a Finnigan MAT 262 thermal ionization mass spectrometer using an ion counter system. Uncertainties of mean age values are given at the 2σ level.

Hf isotope ratios of zircons were obtained on a Nu Instruments multiple collector inductively coupled plasma mass spectrometer (MC-ICPMS; David et al. 2001) at the ETH Zurich, Switzerland. During the analyses, we obtained the $^{176}Hf/^{177}Hf$ ratio of the JMC 475 standard of 0.282141±5 (2 sigma mean) using the $^{179}Hf/^{177}Hf=0.7325$ ratio for normalization. For the calculation of the εHf values, the present day ratios $(^{176}Hf/^{177}Hf)_{CH}=0.28286$ and $(^{176}Lu/^{177}Hf)_{CH}=0.334$ were used, and for 90 Ma, a $^{176}Lu/^{177}Hf$ ratio of 0.0050 for all zircons was taken into account.

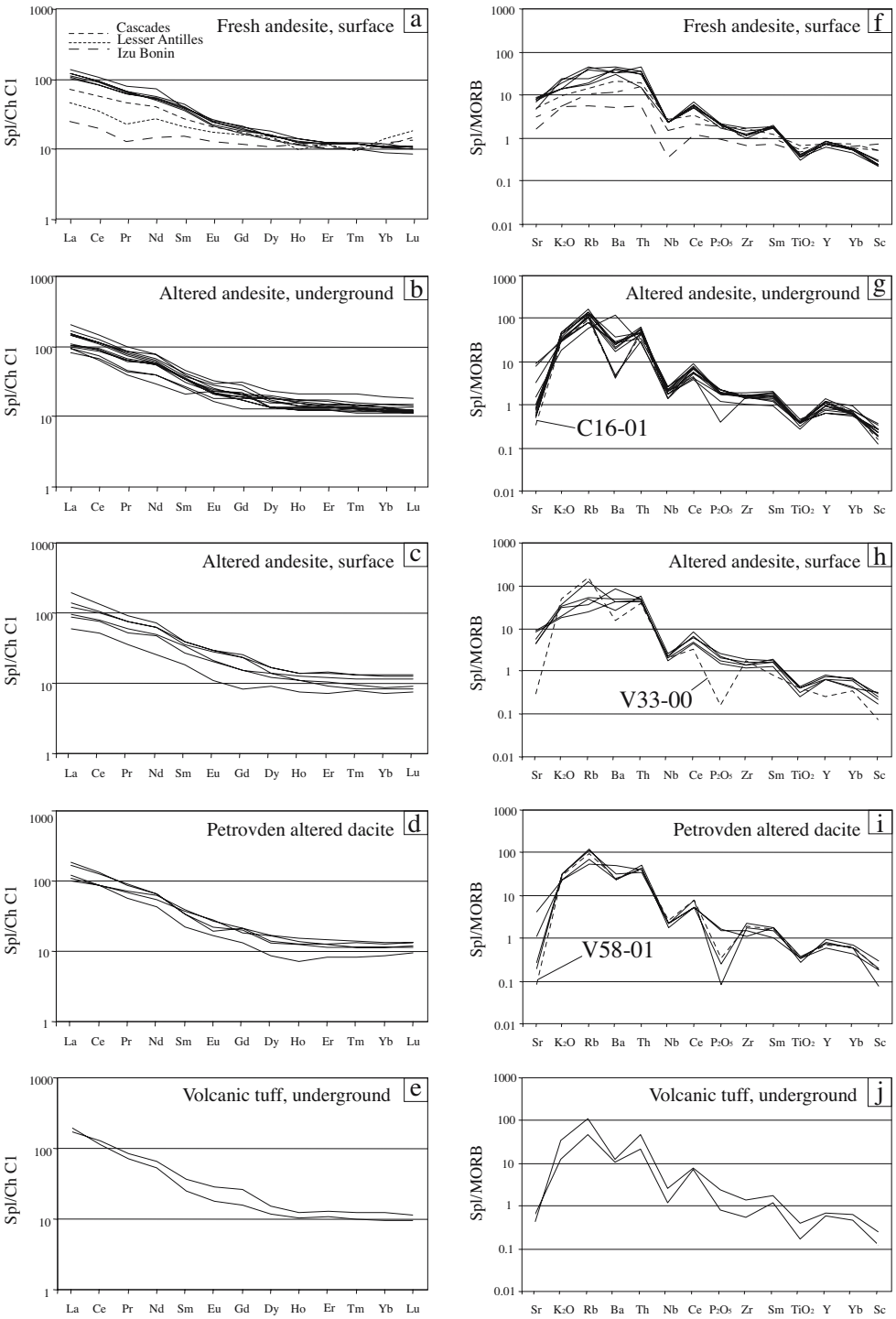

Fig. 9 Chondrite-normalized REE and mid-ocean ridge basalts (MORB)-normalized trace element patterns for the different Chelopech rock types. Chondrite composition from Sun and McDonough (1989), MORB composition from Pearce (1982). C16-01, V33-00, and V58-01 are samples that have been dated

Petrology and geochemistry of magmatic rocks at the Chelopech deposit

Whole rock petrology

We treat only rocks in the immediate vicinity of the Chelopech mine (Fig. 2b,c) and discuss the results in combination with the geochemical and petrological studies of Stoykov et al. (2002, 2004). The different analyzed rock types of the Chelopech area, with characteristic magmatic textures and alteration assemblages, are viewed in thin sections in Fig. 6. Fresh magmatic samples were selected from the two andesitic clast types (AI and AII) of the Vozdol syn-eruptive breccia and andesite of the Chugovitsa syn-volcanic breccia (Figs. 2b, 3; Chambefort 2005). Altered samples from the surface were selected above the mine and in the Petrovden area (Fig. 2b). Underground samples of subvolcanic intrusion and altered volcanic tuff, which host the mineralization, were also analyzed (Fig. 2c).

The andesitic clasts AI and AII of the Vozdol syn-eruptive breccia are porphyritic in texture with a microlitic mesostasis. The phenocrysts are plagioclase (~48 vol.%), amphibole (~10 vol.% in clast AI and ~20 vol.% in clast AII), apatite (~2 vol.%), minor biotite (~1 vol.%), minor titanite (~1 vol.%), and minor magnetite (Fig. 6a,b). The groundmass is composed of finely crystallized plagioclase and quartz. AII clasts include residual corroded quartz phenocrysts (Fig. 6b) and contain rare, entirely crystallized magmatic enclaves identical to those described in the dome-like volcanic body by Stoykov et al. (2002) in the northern part of the Vozdol Valley. Chugovitsa syn-volcanic breccia clasts display the same petrography as clasts AI of the Vozdol breccia. The porphyric texture is preserved in altered samples (Fig. 6c–h). It is important to underscore that biotite, contrary to the other phenocrysts, is systematically altered, even in so-called fresh samples from surface samples. Biotite has an alteration assemblage composed of titanite, quartz, and calcite (Fig. 6c). The alteration minerals grow along the cleavage planes of the relict biotite. In the propylitic zone, alteration minerals such as chlorite, epidote, calcite, and titanite crystallize at the expense of ferromagnesian minerals (Fig. 6d).

Altered magmatic rocks from Petrovden (Fig. 2b) display a residual porphyritic texture with ghosts of plagioclase (~15 vol.%) and amphibole (~3 vol.%) phenocrysts, and subsidiary resorbed quartz (<2 vol.%), essentially replaced by a quartz–sericite alteration assemblage. Figure 6e to g shows the typical texture and mineralogy of samples from the quartz–sericite alteration zone. The porphyritic texture is well preserved, but the magmatic mineral assemblage is completely replaced by sericite, quartz, oxide, and pyrite. Georgieva et al. (2002) also describe alumino–phosphate–sulfate minerals in this alteration zone. In the advanced argillic alteration zone, the original magmatic texture is also preserved (Fig. 6h), even though the rock is composed of a quartz–clay mineral assemblage associated with disseminated pyrite. Pumice and bedding textures are still recognizable in volcanic tuff affected by advanced argillic alteration (Fig. 6i).

Geochemistry of the magmatic rocks at Chelopech

One of the major problems in hydrothermally altered volcanic environments, especially in areas immediately next to the mineralization zone, is to interpret the initial rock composition. At Chelopech, most of the primary mineralogy was partly or totally overprinted by the hydrothermal event. However, some clasts from the Vozdol syn-eruptive breccia (Fig. 2b) are relatively fresh, and combined with published data on magmatic rocks of Stoykov et al. (2002, 2004), it is possible to compare fresh magmatic rock samples from this area with strongly altered rocks within the ore deposit. Preserved volcanic textures, immobile element geochemistry, spider diagrams, and REE patterns have been used to determine the influence of the hydrothermal alteration processes on chemical composition and to classify these rocks. Representative analyses of fresh and altered samples of the Chelopech area are in Table 1; the entire data set can be found in Chambefort (2005). Major and trace element concentrations were recalculated to 100% volatile free and plotted against LOI as a monitor for hydrothermal alteration (Fig. 7).

The SiO_2 concentration of fresh samples varies from 55 to 67 wt%, whereas altered samples have a larger variation from 53 to 80 wt% (Fig. 7a). Alteration processes resulted in leaching of Na_2O and CaO (Fig. 7b,c). In contrast, the altered samples from the underground mine and the surface are enriched in K_2O and Rb (Fig. 7d,e).

The nature of the volcanic to subvolcanic rocks in the Chelopech area was determined using the Nb/Y vs Zr/TiO_2 classification diagram of Winchester and Floyd (1977). The reasonable correlation between TiO_2 (wt%) and Zr (ppm) contents in fresh and altered samples (Fig. 8a) and the absence of any correlation with LOI (Fig. 7f,g) allows us to consider these elements as relatively immobile during the alteration processes. However, the Y content is variable, particularly in the most altered rocks (Fig. 7h). Therefore, the Nb/Y ratio, which corresponds to the alkalinity index (Winchester and Floyd 1977) in Fig. 8b, cannot be considered as a reliable parameter to classify magmatic rocks from the Chelopech area. This problem of classification using Y concentrations and the Winchester and Floyd (1977) diagram has already been noted in previous studies (Finlow-Bates and Stumpfl 1981; Hill et al. 2000). In conclusion, only variations of the Zr/TiO_2 ratio can be confidently used for determining the original magmatic compositions. Except those from the

Petrovden area, the samples plot mostly in the andesite field in the classification diagram of Winchester and Floyd (1977) (Fig. 8b), which is in agreement with preserved andesitic volcanic textures presented in Fig. 5.

In conclusion, the Chelopech magmatic rocks from both surface and underground are similar and have an andesitic composition. The magmatic rocks of the Petrovden area, considered as the altered counterpart of the Murgana dome-

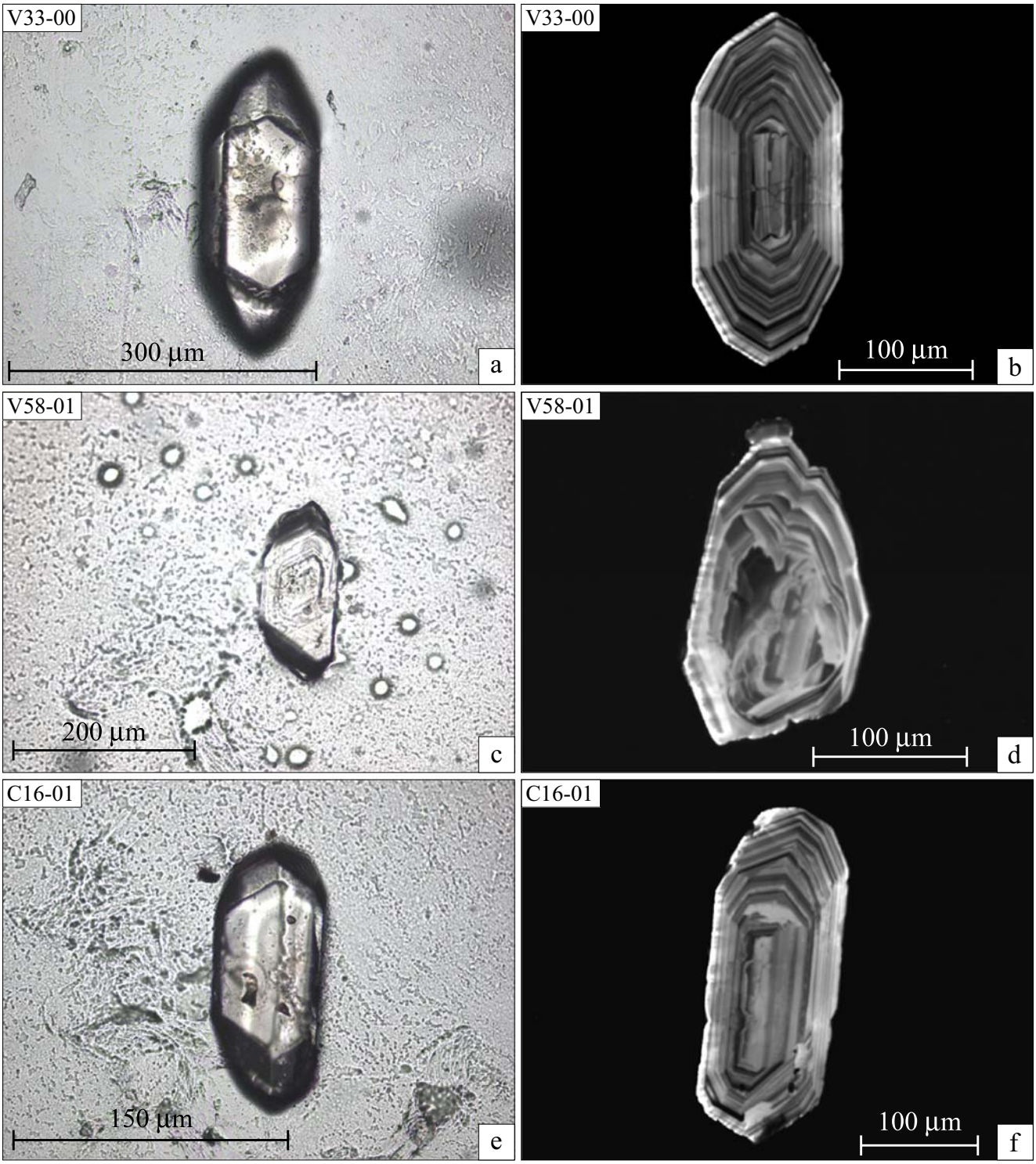

Fig. 10 Characteristic morphology of analyzed zircons. **a**, **c**, and **e** transmitted light. **b**, **d**, and **f** cathodoluminescence pictures. **a**, **b** Sample V33-00; **c**, **d** sample V58-01, and **e**–**f** sample C16-01

Table 2 U–Pb zircon isotope data for the Chelopech magmatic rocks—samples V33-00, V58-01, and C16-01

N	Sample/size fraction (μm)	Weight (mg)	Type	U	Pb	$^{206}Pb/^{204}Pb$	$^{206}Pb/^{238}U$	2σ Error	$^{207}Pb/^{235}U$	2σ Error	$^{207}Pb/^{206}U$	2σ Error	$^{206}Pb/^{238}U$	$^{207}Pb/^{235}U$	$^{207}Pb/^{206}U$	Rho[a]
				ppm									Apparent ages			
	V33-00															
1	Zircon 2752	0.0246	abr.	164.1	2.668	941.1	0.01478	0.00007	0.09819	0.00056	0.04812	0.00013	94.57	95.11	108.6	0.88
2	Zircon 2753	0.0163	abr.	169.7	2.828	457.5	0.01453	0.00008	0.09601	0.00078	0.04793	0.00026	92.98	93.09	95.85	0.74
3	Zircon 2754	0.0244	abr.	135.0	2.194	681.3	0.01444	0.00011	0.09515	0.00076	0.04777	0.00015	92.44	92.29	88.3	0.92
4	Zircon 2755	0.0116	abr.	181.5	2.942	667.1	0.01431	0.00006	0.09484	0.00065	0.04805	0.00023	91.63	92.01	101.8	0.71
5	Zircon 2756	0.0045	abr.	499.1	7.882	637.5	0.01442	0.00007	0.09548	0.00064	0.04802	0.00019	92.29	92.59	100.4	0.82
	V58-01															
6	Zircon 2760	0.0080	abr.	292.6	15.41	1532.7	0.04982	0.00027	0.36147	0.00246	0.05261	0.00020	313.4	313.3	312.3	0.82
7	Zircon 2762	0.0013	abr.	226.2	9.509	1938.3	0.03966	0.00018	0.30767	0.00148	0.05626	0.00006	250.7	272.4	462.7	0.98
8	Zircon 2763	0.0014	abr.	110.2	6.229	2969.3	0.05636	0.00028	0.43808	0.00228	0.05637	0.00006	353.5	368.9	467.1	0.97
9	Zircon 2758	0.0082	abr.	203.3	3.459	425.5	0.01433	0.00007	0.09501	0.00079	0.04807	0.00031	91.75	92.16	102.63	0.62
10	Zircon 2761	0.0033	abr.	279.6	4.706	450.6	0.01439	0.00007	0.09424	0.00094	0.04747	0.00039	92.15	91.44	72.96	0.57
11	Zircon 2759	0.0045	non abr	282.9	4.258	179.1	0.01390	0.00006	0.09222	0.00082	0.04812	0.00034	88.98	89.57	105.2	0.59
	C16-01															
12	Zircon 2640	0.0078	abr.	128.6	2.438	244.6	0.01428	0.00010	0.09435	0.00358	0.04792	0.00168	91.41	91.55	95.33	0.44
13	Zircon 2641	0.0116	abr.	149.2	2.427	532.2	0.01426	0.00008	0.09492	0.00159	0.04827	0.00072	91.29	92.08	112.5	0.46
14	Zircon 2642	0.0012	abr.	199.1	3.534	290.1	0.01432	0.00008	0.09487	0.00256	0.04805	0.00122	91.66	92.03	101.7	0.43
15	Zircon 2643	0.0007	abr.	177.2	3.031	387.7	0.01428	0.00011	0.09630	0.00250	0.04888	0.00117	91.45	93.35	142.3	0.44
16	Zircon 2638	0.0149	abr.	194.1	3.342	337.1	0.01406	0.00031	0.09545	0.00534	0.04923	0.00241	90.02	92.57	158.9	0.50
17	Zircon 2639	0.0004	non abr	268.7	5.982	129.6	0.01378	0.00009	0.09203	0.00322	0.04842	0.00136	88.25	89.39	120.1	0.58

abr. Abraded, *non abr* non abraded

[a] Correlation coefficient $^{206}Pb/^{238}U$–$^{207}Pb/^{235}U$

like body defined by Stoykov et al. (2002) (Fig. 2a), have a more dacitic composition.

Rare earth elements and spider diagrams

REE patterns and spider diagrams are shown in Fig. 9. Five groups of samples are presented, which have been delimited by their geographical position and their lithologies. Fresh rock compositions from the Vozdol and Chugovitsa syn-volcanic breccia (Fig. 2b) with an andesitic composition are shown in Fig. 9a. In comparison, altered andesite from underground subvolcanic bodies (Fig. 9b), altered andesitic rock from surface outcrops directly above the mine (Fig. 9c), altered dacitic rock from the Petrovden zone (Figs. 2b and 9d), and underground altered volcanic tuff (Fig. 9e) have been plotted in different diagrams for the sake of clarity.

All rocks have decreasing light REE and relatively flat heavy REE patterns and are typical of subduction-related volcanic rocks (Pearce 1982). No significant Eu anomaly is present in the REE spectra, suggesting that there is no extensive plagioclase fractionation involved in the genesis of these rock types.

Trace element spider diagrams exhibit some variations between fresh and altered rock samples: Fresh magmatic rocks (Fig. 9f) display negative anomalies in large ion, lithophile elements (Sr, K, Rb, and Ba) and high field strength elements (Nb, Ti, and Zr), characteristic of subduction-related magmatic rocks (Pearce 1982).

Altered hypabyssal bodies with preserved andesitic texture, sampled underground and on surface (Fig. 9g–i), are depleted in Sr and P_2O_5 compared to fresh andesitic rocks (Fig. 9f) and are enriched in K_2O and Rb. Sr, K_2O, Ba, Y, and P_2O_5 are strongly mobile elements during the alteration processes. TiO_2, Nb, and Zr appear to be immobile during the hydrothermal alteration, while the variable Ba concentration can be related to the presence or absence of barite in the alteration assemblages. Volcanic tuff (Fig. 9j) displays similar patterns to those of altered andesitic rock.

Geochronological studies of the Chelopech deposit

Previous geochronological studies in the Chelopech area were designed to unravel the magmatic evolution (Handler

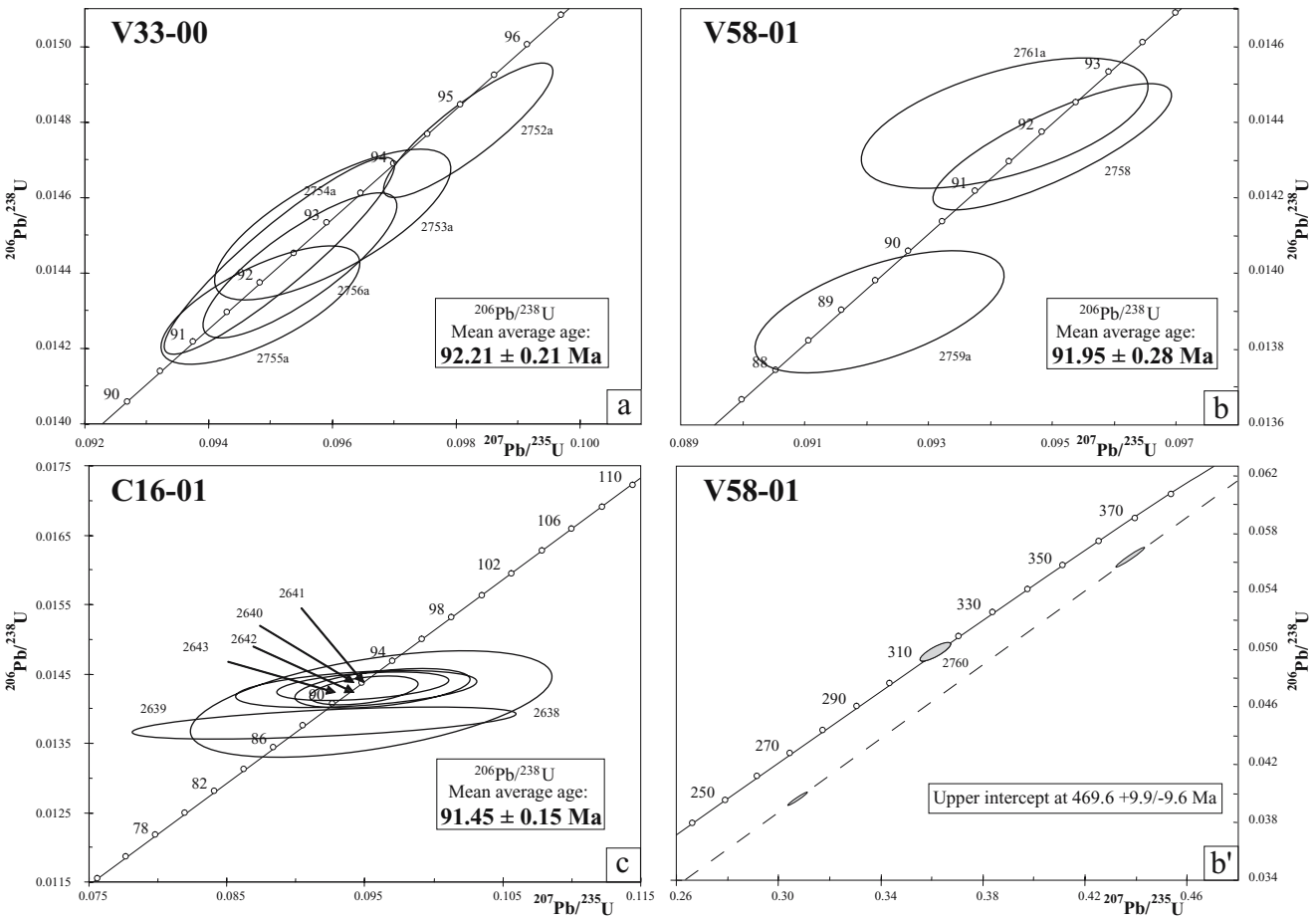

Fig. 11 U–Pb concordia diagram. **a** The altered magmatic rock on surface V33-00. **b** and **b′** The altered dacite dome-like body of the Petrovden zone V58-01. **c** The altered andesite subvolcanic body, which hosts the high-sulfidation epithermal Chelopech deposit C16-01

Table 3 Hf zircon isotope data for magmatic rocks of the Chelopech deposit

Sample	$^{176}Hf/^{177}Hf$	2σ Error	εHf today	$εHf_{T90}$ (Ma)
V33-00				
2754	0.282760	0.000003	−0.42	1.06
2753	0.282731	0.000003	−1.45	0.04
2755	0.282737	0.000003	−1.24	0.25
2752	0.282760	0.000002	−0.42	1.06
2757	0.282760	0.000005	−0.42	1.06
V58-01				
2760	0.282565	0.000003	−7.32	−5.84
2762	0.282836	0.000003	2.26	3.75
2761	0.282852	0.000004	2.83	4.32
2763	0.282684	0.000004	−3.11	−1.63
2758	0.282852	0.000004	2.83	4.32
2759	0.282840	0.000009	2.40	3.89
C16-01				
2637	0.282774	0.000005	0.07	1.56
2638	0.282774	0.000010	0.07	1.56
2641	0.282751	0.000004	−0.74	0.74

^{176} Hf/^{177} Hf analyses, ETH—Zurich

et al. 2004; Stoykov et al. 2004; Figs. 2a and 3). In this study, we focus on dating the immediate host and country rocks of the Chelopech deposit, to constrain the age of formation of the high-sulfidation epithermal deposit with respect to local magmatism and, more regionally, to porphyry–Cu ore formation and magmatism at Elatsite, located 6 km to the northwest (Fig. 2a).

Sample V33-00

This sample comes from altered rocks just above the Chelopech underground mine (Fig. 2b,c). It is characterized by argillic alteration. Clay minerals and sericite replace plagioclase phenocrysts of the initial porphyritic texture. Hydrothermal quartz is crystallized in the mesostasis, with anatase and minor alumino–phosphate–sulfate minerals. Zircon is relatively abundant. Oscillatory zoning is typical of magmatic zircons (Fig. 10a,b); grains are pink, euhedral, prismatic, and are ~50 to 400 μm long.

Sample V58-01

This quartz–sericite altered sample comes from an outcrop on the Petrovden peak (Fig. 2b). It is a sample of the altered part of the Murgana dacitic dome-like body defined by Stoykov et al. (2002). This rock has preserved porphyritic texture with resorbed quartz phenocrysts (Fig. 6e). Plagioclase phenocrysts are totally replaced by sericite and minor hydrothermal quartz. The mesostasis is composed of a very fine assemblage of sericite and quartz. Hydrothermal anatase is also present and has incorporated Ti released

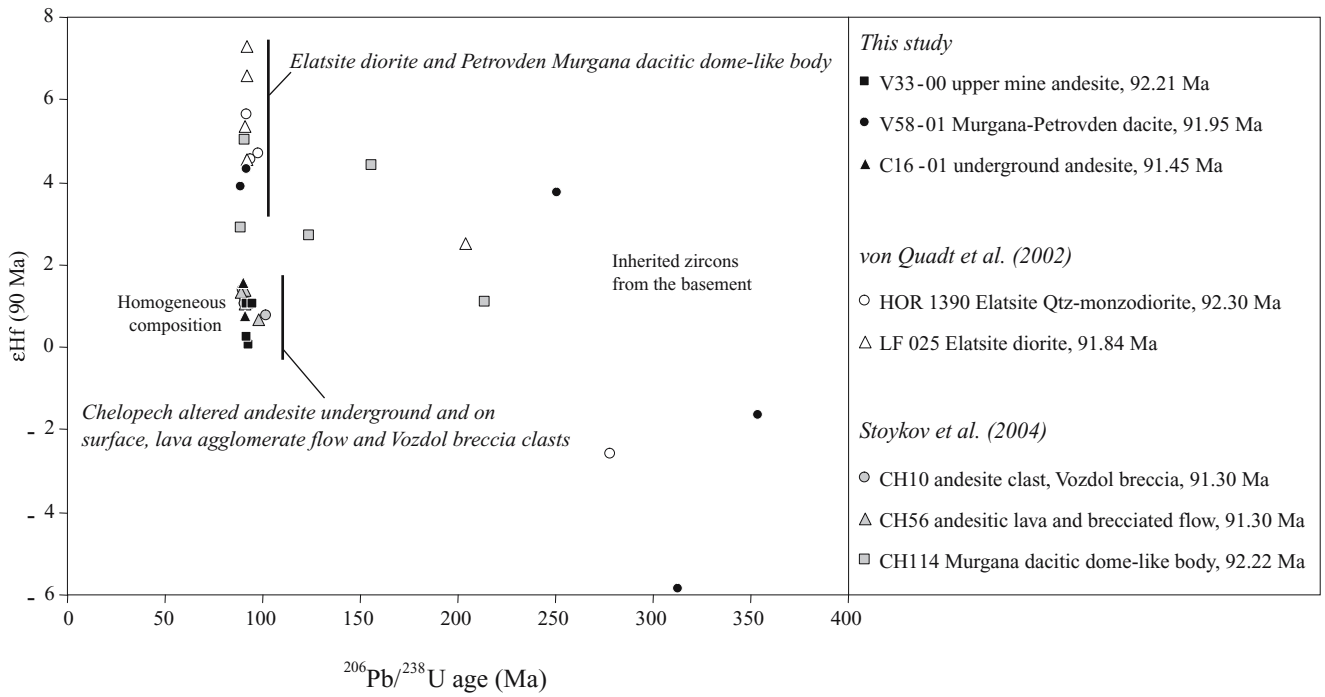

Fig. 12 εHf values calculated for 90 Ma vs $^{206}Pb/^{238}U$ apparent ages. *Black symbols*, this study, V33-00: altered andesite upper mine (mean average age 92.21±0.21 Ma), V58-01: Petrovden Murgana dacitic body (91.95±0.28 Ma), C16-01: altered andesite in the mine hosting the mineralization (91.45±0.15 Ma). *Open symbols*, data for the Elatsite porphyry–Cu from von Quadt et al. (2002), HOR 1390: "big dyke" Unit 1, quartz–monzodiorite porphyry (92.10±0.30 Ma), LF 025: Unit 2, diorite porphyry (91.84±0.31 Ma). *Gray symbols*, Chelopech magmatic rocks area from Stoykov et al. (2004), CH10: Unit 3, andesitic clast of the Vozdol breccia (91.30±0.30 Ma), CH56: Unit 2, lava and agglomerate flow northern part of Chelopech (91.30±0.30 Ma), and CH114: Unit 1, trachydacite of the Murgana dome-like body (92.22±0.30 Ma)

during alteration of magmatic ferromagnesian minerals. Zircon grains are of two types: prismatic (Fig. 10c,d) and rounded-prismatic and are typically ~40 to 250 μm long. Cathodoluminescence shows that rounded-prismatic zircons have a cloudy core surrounded by a layer with oscillatory zoning (Fig. 10d), which can be interpreted as an inherited zircon core.

Sample C16-01

This sample comes from the exploitation block 18 on level 405 of the mine and represents the hypabyssal body with an andesitic texture, which is the immediate host of the mineralization (Fig. 2c). It displays argillic alteration associated with disseminated pyrite. A relic porphyry texture can still be recognized despite the intense alteration. As in the other dated samples, zircon grains are very abundant. Crystals are prismatic with ~160 to 220 μm in size. As for sample V33-00, cathodoluminescence shows oscillatory zoning typical of magmatic zircons (Fig. 10e,f).

U–Pb geochronology

U–Pb zircon isotope data are reported in Table 2. Five zircons were separated and analyzed from sample V33-00 and reported on a $^{206}Pb/^{238}U$ vs $^{207}Pb/^{235}U$ concordia diagram (Fig. 11a). Zircons 2753, 2754, 2755, and 2756 define a calculated concordant $^{206}Pb/^{238}U$ age of 92.21±0.21 Ma (Ludwig 1999). This age is interpreted as the formation age of the hypabyssal andesite. Zircon 2752 displays a minor proportion of inherited lead and is not included in the calculation. The abraded zircons have a wide range of U contents from 135.0 to 499.1 ppm, and the Pb contents in the same grains range from 2.194 to 7.882 ppm.

Two out of six zircons analyzed from sample V58-01 of the Petrovden dacitic dome-like body, are concordant and display a mean $^{206}Pb/^{238}U$ age of 91.95±0.28 Ma (2758, 2761, Table 2, Fig. 11b). This age overlaps within uncertainties with the age of 92.22±0.30 Ma obtained by Stoykov et al. (2004) for the Murgana dacitic dome-like body (Figs. 2b and 5). One zircon grain has a larger proportion of inherited lead (2763, Table 2), yielding an age of 313.4±1.6 Ma. Two zircon grains are discordant and define an upper intercept at 469.6 +9.9, −9.6 Ma (Fig. 11b′). This discordia age is interpreted as an assimilation of Paleozoic crustal material, in agreement with cathodoluminescence showing the presence of inherited cores (Fig. 10d). The zircon has a range of U contents from 110.2 to 292.6 ppm and Pb contents from 3.459 to 15.410 ppm. A non-abraded zircon grain (2759, Table 2, Fig. 11b′) displays a minor proportion of inherited lead, characterizing lead loss during evolution with time.

Six zircons of sample C16-01 were analyzed and are all concordant. Only four of them were used to define a mean $^{206}Pb/^{238}U$ age of 91.45±0.15 Ma (2643, 2642, 2640, 2641, Table 2, Fig. 11c). A non-abraded zircon (2639, Table 2, Fig. 11c) shows minor inherited lead and was not used in the calculation. Zircon 2638 displays an important error and was also not used to determine the mean age. This age of 91.45±0.15 Ma is interpreted as the intrusion age of the subvolcanic body, which hosts the mineralization underground. The abraded zircons have a wide range of U contents from 128.6 to 199.1 ppm, and the Pb contents in the same grains range from 2.427 to 3.534 ppm.

Hf isotopes

Zircons of the andesitic body sampled on surface just above the mine (V33-00, in Fig. 2b) yield a range of εHf recalculated at 90 Ma from 0.04 to 1.06 (Table 3). The Petrovden zircon samples (V58-01, in Fig. 2b) have εHf values that vary from −5.84 to 4.32. There is a correlation between the incorporation of an increasing old lead component with low $^{176}Hf/^{177}Hf$ ratios (Fig. 12). The zircons with the highest proportion of an old component have the lowest εHf value. Sample C16-01 (Fig. 2c) has εHf values that range from 0.74 to 1.56.

Samples C16-01 and V33-00 display almost the same range of εHf values between 0.04 and 1.56 (Fig. 12). These values are characteristic of a mixed crustal and mantle origin for the magma and define the same magma source for both magmatic units.

In contrast, zircons from dacitic rocks of the Petrovden area (Fig. 2b) have a large variation of $^{176}Hf/^{177}Hf$ ratios.

Table 4 Age and Hf isotope differences between Petrovden and Chelopech magmatic rocks

	Petrovden		Chelopech
Composition	Dacite, dome-like body		Andesite, subvolcanic, lava flow, synvolcanic breccia
εHf_{T90}	−5.84→3.75	3.89→4.32	0.04→1.06
Interpretation	Inherited lead from old basement rocks	Mantellic component	Mixed crustal–mantle source
Ages (U–Pb) (This study; Stoykov et al. 2004)	469.6+9.9, −9.6 Ma 313.4±1.6 Ma	92.22±0.30 Ma	92.21±0.21→91.30±0.30 Ma

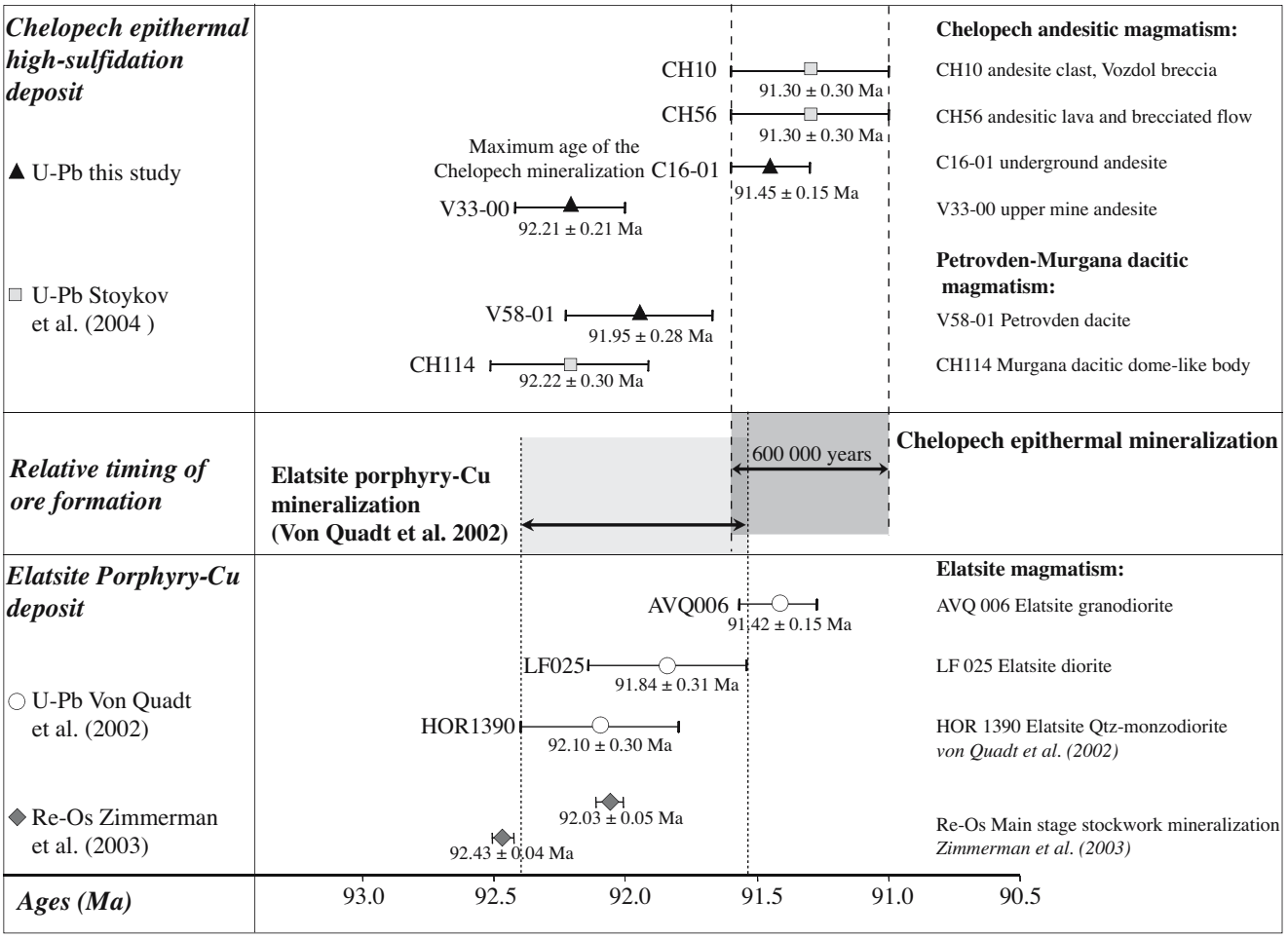

Fig. 13 Compilation of age data on the Chelopech high-sulfidation epithermal and Elatsite porphyry–Cu deposits

Old lead enriched zircons have the lowest εHf values, which are characteristic of the assimilation of a crustal component, whereas youngest zircons display εHf values with a more predominant mantellic component in the magma source (Fig. 12).

Discussion and conclusions

Evolution and geochronology of magmatism at Chelopech

The Chelopech magmatic rocks are relatively homogeneous and display similar geochemical variations. REE and trace element patterns are typical of subduction-related volcanism. Our whole-rock analyses of the magmatic rocks, which host the Chelopech deposit, are in agreement with the recent petrological study of Stoykov et al. (2002) and indicate a calc-alkaline andesitic to dacitic (Petrovden member) composition. In addition, Stoykov et al. (2002) describe shoshonitic compositions and high-K volcanic rocks. We have shown that K_2O and Na_2O are strongly mobile in the hydrothermal area, even in so-called fresh magmatic rocks (Fig. 7). Therefore, Na_2O+K_2O vs SiO_2 or K_2O vs SiO_2 (wt%) diagrams (Le Maître 1989; Stoykov et al. 2002) must be used with caution. The presence of plagioclase associated with amphibole and biotite phenocrysts shows that the H_2O content in the magma was higher than 1.5 wt% (Thorpe 1982).

Figure 12 displays the εHf data of magmatic rocks from the Chelopech and Petrovden areas obtained in this study and by Stoykov et al. (2004), which are compared to data of magmatic rocks from the Elatsite porphyry–Cu deposit area (von Quadt et al. 2002), and Table 4 contrasts the different characteristics of the Petrovden dacite and the Chelopech andesite. It appears that the Hf isotope data can be subdivided into two groups. A fairly homogeneous group of data with εHf of 0.04 to 1.56 for ages at approximately 91–92 Ma is exhibited by the underground subvolcanic andesitic body at Chelopech (C16-01, in Fig. 2c), altered andesite located on surface immediately on top of the mine (V33-00, Fig. 2b,c), lava and brecciated flow, and clasts from the Vozdol lava breccia (CH56, CH10 in Fig. 2a, Stoykov et al. 2004). Such εHf values are characteristic of a mixed crust–mantle source.

In contrast, samples from the Murgana–Petrovden dacitic dome-like body (V58-01 in Fig. 2b, CH114 in Fig. 2a, Stoykov et al. 2004) display higher εHf values, which range from 2.90 to 5.02 for the same age range and which overlap with the εHf values of intrusive rocks at the porphyry–Cu deposit of Elatsite (von Quadt et al. 2002). These isotopic compositions are typical of a predominantly mantle source. The correlation of decreasing εHf values with older zircon ages reveals the incorporation of an old lead component in the magma that produced the dome-like body at Petrovden (Murgana) and the intrusive rocks at Elatsite (Fig. 12). The old lead component can be explained by assimilation of metamorphic basement rocks by the magma, which is supported by inherited cores in the zircons (Fig. 10d). The upper intercept in the $^{206}Pb/^{238}U$ vs $^{207}Pb/^{235}U$ concordia diagram (Fig. 11b′) shows an age of 469.6+9.9/−9.6 Ma, which closely corresponds to the age of the Paleozoic basement rocks in the region (von Quadt et al. 2002). Nd isotopic data of magmatic rocks agree with this interpretation, with εNd (T=90 Ma) values of −0.03 and 2.27 at the Elatsite porphyry–Cu deposit (von Quadt et al. 2002) and values between −3.55 and −2.27 at Chelopech (Stoykov et al. 2004) revealing a higher mantle component in magmatic rocks at Elatsite in comparison to Chelopech.

Our U–Pb geochronological results show that andesitic rocks thrust over on the Chelopech deposit (sample V33-00, Fig. 2c) have the same age as the Petrovden dacite (V58-01, Fig. 2b) dated by Stoykov et al. (2004) and the intrusive rocks hosting the Elatsite porphyry–Cu deposit (Fig. 13). This reveals that the Murgana–Petrovden dacitic dome-like body, intrusive activity at Elatsite, and early andesitic volcanism at Chelopech were contemporaneous, within resolution of radioisotopic age determinations. This also indicates that two physically distinct upper crustal, magmatic reservoirs with different compositions were coexisting at about 92 Ma, with a mantle-dominated magmatic source mixed with older crustal basement material in the north, responsible for the magmatism at Murgana–Petrovden and Elatsite, and a more homogeneous source reservoir with both mantle and young crustal material but without any assimilation of old crustal basement material that generated the andesitic magmatism at Chelopech in the south. Therefore, the north-to-south (Elatsite to Chelopech) decrease in the mantle and old crustal basement components cannot be simply explained by a simple magma evolution over time of the same magmatic reservoir. However, our data do not allow us to state whether both coexisting upper crustal magma reservoirs were linked to a single, large magmatic chamber at depth or whether they were distinct magma systems. The regional geomagnetic anomaly recognized below the Elatsite–Chelopech ore deposit cluster by Popov et al. (2001) tends to support the former interpretation, i.e. a single magmatic chamber at depth, in which variable degrees of mixing may have produced the compositional differences observed between the magmatic rocks at Elatsite and Chelopech.

The latest magmatic stage is the Vozdol breccia, as dated at 91.30±0.30 Ma by Stoykov et al. (2004, U–Pb age on zircon) on an andesitic clast (sample CH10 in Fig. 2a), which has a magmatic texture and chemical composition corresponding to the AI clast type from the Vozdol syn-volcanic breccia (Stoykov 2005, personal communication). This age interpretation is consistent with all field studies, whether one accepts the interpretation by Popov and Kovachev (1996), Popov and Popov (2000), and Popov et al. (2000) suggesting that this breccia is a late volcanic neck or our interpretation suggesting that it is a resedimented and syn-eruptive breccia as based on our recent field observations (see above; Fig. 3; Chambefort 2005). The U–Pb data show that andesitic magmatism at Chelopech outlasted the dacitic magmatism of the Murgana–Petrovden area (Fig. 12).

Age of the Chelopech high-sulfidation epithermal deposit and duration of the hydrothermal event

The hypabyssal andesitic body overprinted by hydrothermal alteration at Chelopech yields a U–Pb age of 91.45±0.15 Ma (sample C16-01 in Figs. 2c, 5, and 13). Therefore, its U–Pb zircon age defines a maximum age for the Chelopech epithermal high-sulfidation deposit. The Vozdol breccia constitutes the last magmatic event at Chelopech dated at 91.30±0.30 Ma (Stoykov et al. 2004). If we accept that the occasional altered volcanic clasts in the Vozdol breccia belong to the same hydrothermal alteration event associated with the Chelopech high-sulfidation deposit (Georgieva et al. 2004), then the magmatic age of the Vozdol breccia also defines a minimum age of Chelopech deposit and permits us to bracket its genesis between 91.45±0.15 and 91.30±0.30 Ma. Therefore, given the analytical uncertainties, ore formation took place between a maximum age of 91.6 Ma and a minimum age of 91.0 Ma (Fig. 13), which narrows the maximum duration of ore formation at Chelopech down to 600,000 years. However, the origin of the altered clasts in the Vozdol breccia is not definitely solved and cannot be attributed unambiguously to the Chelopech alteration, as other alteration zones with unknown age relationships, such as Petrovden, are also recognized (Fig. 4a,b). Therefore, the presence of the altered clasts in the Vozdol breccia described by Georgieva et al. (2004) must still be viewed cautiously as evidence for a minimum age limit of the Chelopech deposit.

Relationship of the Chelopech epithermal and Elatsite porphyry–Cu deposits during the evolution of the northern Panagyurishte district

Recent U–Pb zircon data on the Elatsite deposit (von Quadt et al. 2002) demonstrate that the porphyry–Cu deposit was formed between 92.10±0.30 and 91.84±0.31 Ma (Figs. 5 and 13). As discussed above, the Chelopech high-sulfidation epithermal deposit is younger than 91.45±0.15 Ma, and the hydrothermal activity related to this deposit ceased by 91.30 ±0.30 Ma according to Stoykov et al. (2004) and Georgieva et al. (2004). Thus, the high-sulfidation epithermal deposit is slightly younger than the porphyry–Cu deposit; however, both deposits have very close ages and were formed within less than 1.4 Ma. Within the uncertainties of the individual U–Pb ages, the early stages of ore formation at the Chelopech high-sulfidation epithermal deposit may have been contemporaneous with the waning ore formation stages at the Elatsite porphyry–Cu deposit (Fig. 13).

Based on Hf isotope systematic, andesitic magmatic rocks predating (underground andesite, sample C16-01 in Figs. 12 and 13) and postdating (Vozdol breccia, sample CH10 in Figs. 12 and 13) the emplacement of the Chelopech epithermal deposit were sourced by a mixed crustal–mantle reservoir, whereas the magmatic rocks hosting the 6-km distant Elatsite porphyry–Cu deposit are predominantly of mantle origin. U–Pb geochronology also indicates that the two physically distinct magmatic reservoirs were coexisting (Fig. 13), arguing against an evolution over time of a single magmatic reservoir. Therefore, we conclude that the magmatic–hydrothermal systems forming the Chelopech and Elatsite deposits were related to distinct, shallow crustal intrusions. Although, as stated earlier, they could both be related to a single magmatic chamber at depth as Popov et al. (2001) concluded based on geophysical data.

Genetic models typically suggest that paired porphyry–Cu and high-sulfidation epithermal deposits form from a single magmatic–hydrothermal system centered on the same, upper crustal intrusion (e.g. Hedenquist and Lowenstern 1994; Arribas et al. 1995; Heinrich et al. 1999). Thus, if the above-mentioned interpretation is accepted, this may have important implications for mineral exploration, as there would still be open ground at depth at Chelopech for exploration of a porphyry–Cu deposit expected to be genetically paired with the epithermal high-sulfidation deposit. By contrast, any high-sulfidation deposit that would have been paired with the Elatsite porphyry–Cu deposit would have been eroded. According to our interpretation, the Elatsite porphyry–Chelopech epithermal association would be comparable to the relationship recognized for instance in the Collahuasi district, Chile, where early porphyry–Cu formation and subsequent high-sulfidation epithermal mineralization were related to two adjacent but physically and temporally distinct shallow level intrusions (see Fig. 21 in Masterman et al. 2005). Such a genetic scenario is distinct from cases such as Lepanto, Philippines (Arribas et al. 1995; Hedenquist et al. 1998), where the porphyry–Cu and high-sulfidation epithermal deposits were formed within a single magmatic–hydrothermal system, centered on a single, shallow magmatic intrusion.

The tight clustering of magmatism and ore formation in the Chelopech–Elatsite area at about 91–92 Ma fits into the regional north-to-south younging of magmatism and ore formation in the Panagyurishte district, related to slab rollback by von Quadt et al. (2005a). von Quadt et al. (2005a) also argue, based on radiogenic isotopes, for an evolution during slab rollback from a predominantly mixed crust–mantle source in the northern Panagyurishte district to magmas with a higher mantle component in the southern part. Our study within the northern Panagyurishte district shows that on a local, more detailed scale, both types of magma sources can be present and can be coeval, within analytical uncertainties. Thus, during the tectono–magmatic evolution of the Panagyurishte district, petrogenesis was certainly more complex, than within a simple slab rollback setting, and other additional, more local processes must have operated during magma formation.

Acknowledgements This study is dedicated to Dr. Rumen Petrunov. This work was supported by the Swiss Science Foundation through the research grants 21-59041.99 and 200020-101853 and the SCOPES Joint Research Project 7BUPJ62276.00/1. S. Stoykov (University of Mining and Geology, Sofia) is gratefully acknowledged for his discussion and data, S. Georgieva is acknowledged for the surface alteration data and S. Jacquat and R. Petrunov for joint fieldwork. The authors would like to thank P. Voldet for REE analyses at the University of Geneva, F. Caponi for the major and trace element X-ray fluorescence analyses, and M. O. Diserens for cathodoluminescence images. The authors would like to thank the staff of the Geology Department from the Chelopech Mine for arranging access to the mine and sharing geological information. Prof. Anita Grunder (Oregon State University) is acknowledged for revision of the manuscript. This is a contribution to the ABCD–GEODE research program supported by the European Science Foundation.

References

Aiello E, Bartolini C, Boccaletti M, Gocev P, Karagjuleva J, Kostadinov V, Manetti P (1977) Sedimentary features of the Srednogorie zone (Bulgaria): an Upper Cretaceous intra-arc basin. Sediment Geol 17:39–67

Arnaudov V, Amov B, Bratnitzkii B, Pavlova M (1989) Isotopic geochronology of magmatic and metamorphic rocks from Balkanides and Rhodopes massif. Proceedings, XIV Congress of the

Carpathian–Balkan Geological Association, Sofia, pp 1154–1157 (in Russian)
Arribas A Jr, Hedenquist JW, Itaya T, Okada T, Conception RA, Garcia JS Jr (1995) Contemporaneous formation of adjacent porphyry and epithermal Cu–Au deposits over 300 ka in northern Luzon, Philippines. Geology 23:337–340
Berza T, Constantinescu E, Vlad SN (1998) Upper Cretaceous magmatic series and associated mineralisation in the Carpathian–Balkan Orogen. Resour Geol 48:291–306
Boccaletti M, Manetti P, Peccerillo A, Stanisheva-Vassileva G (1978) Late Cretaceous high-potassium volcanism in Eastern Srednogorie, Bulgaria. Geol Soc Amer Bull 89:439–447
Carrigan CW, Mukasa SB, Haydoutov I, Kolcheva K (2005) Age of Variscan magmatism from the Balkan sector of the orogen, central Bulgaria. Lithos 82:125–147
Cathles LM, Erendi AHJ, Barries T (1997) How long can a hydrothermal system be sustained by a single intrusive event? Econ Geol 92:766–771
Chambefort I (2005) The Cu–Au Chelopech deposit Panagyurishte district, Bulgaria: volcanic setting, hydrothermal evolution and tectonic overprint of a Late Cretaceous high-sulfidation epithermal deposit. Ph.D. thesis, University of Geneva, Terre et Environnement, vol 52, p 173
Chambefort I, Moritz R (2006) Late Cretaceous structural control and Alpine overprint of the high-sulfidation Cu–Au epithermal Chelopech deposit, Srednogorie belt, Bulgaria. Miner Depos 41:259–280
Chambefort I, Moritz R, Jacquat S, Petrunov R (2003) Influence of the volcanic environment on hydrothermal fluids circulation: example of the Chelopech Au–Cu high-sulfidation epithermal deposit, Bulgaria. XXIII General assembly of IUGG, Sapporo, Japan, abstract volume, V07/03A/A01-008, A520
Cheshitev G, Milanova V, Sapounov I, Choumachenko P (1995) Explanatory note to the geological map of Bulgaria in scale 1:100 000, Teteven map sheet, Avers, Sofia (in Bulgarian)
Chipchakova S, Lilov P (1976) Absolute ages of Upper Cretaceous magmatism in the Western part of the Central Srednogorie and related ore-mineralization. Comptes rendus de l'Académie Bulgare des Sciences 29:101–104 (in Russian)
Ciobanu CL, Cook NG, Stein H (2002) Regional setting and Re–Os age of ores at Ocna de Fier Dognecea (Romania) in the context of the banatitic magmatic and metallogenic belt. Miner Depos 37:541–567
Corbett GJ, Leach TM (1998) Southwest Pacific Rim gold–copper systems: structure, alteration, and mineralization. Soc Econ Geol Spec Publ 6:237
Dabovski C (1988) Precambrian in the Srednogorie zone (Bulgaria). In: Cogne J, Kozhoukharov D, Krautner HG (eds) Precambrian in younger fold belts. Wiley, Essex, pp 841–847
Dabovski C, Zagorchev I, Rouseva M, Chounev D (1972) Paleozoic granitoids in the Sushtinska Sredna Gora. Annual UGP 16:57–92 (in Bulgarian)
Dabovski C, Harkovska A, Kamenov B, Mavrudchiev B, Stanisheva-Vassileva G, Yanev Y (1991) A geodynamic model of the Alpine magmatism in Bulgaria. Geol Balk 21:3–15
David K, Frank M, O'Nions RK, Belshaw NS, Arden JW (2001) The Hf isotope composition of global seawater and the evolution of Hf isotopes in the deep Pacific Ocean from Fe–Mn crusts. Chem Geol 178:23–42
Finlow-Bates T, Stumpfl EF (1981) The behaviour of so-called immobile elements in hydrothermally altered rocks associated with volcanogenic submarine-exhalative ore deposits. Miner Depos 16:319–328
Foose RM, Manheim F (1975) Geology of Bulgaria: a review. AAPG Bull 59:303–335
Georgiev N, Ivanov Z (2003) Magma mixing and emplacement of plutonic bodies: an example from the southern part of the Panagyurishte ore district. In: Bogdanov K, Strashimirov S (eds) Cretaceous porphyry epithermal systems of the Srednogorie zone, Bulgaria. Soc Econ Geol Guidebook 36:115–118
Georgieva S, Velinova N, Petrunov R, Moritz R, Chambefort I (2002) Aluminium phosphate–sulfate minerals in the Chelopech Cu–Au deposit: spatial development, chemistry and genetic significance. Geochem Miner Petrol 39:39–51
Georgieva S, Petrunov R, Moritz R, Stoykov S, Peytcheva I, von Quadt A (2004) Temporal relationship between volcanism and the hydrothermal system in the region of Chelopech high-sulfidation Cu–Au deposit: constraints from geochronological and mineralogical data. Bulgarian geological society, annual scientific conference, "geology 2004," pp 21–23
Handler R, Neubauer F, Velichkova SH, Ivanov Z (2004) $^{40}Ar/^{39}Ar$ age constraints on the timing of magmatism and post-magmatic cooling in the Panagyurishte region, Bulgaria. Swiss Bull Miner Petrol 84:119–132
Haydoutov I (1987) Ophiolites and island-arc igneous rocks in the Caledonian basement of the South Carpathian–Balkan region. In: Flügel H, Sassi FP Grecula P (eds) Pre-Variscan and Variscan events in the Alpine–Mediterranean mountain belts. Mineral Slov, Spec Monograph, pp 279–292
Haydoutov I (2001) The Balkan island-arc association in west Bulgaria. Geol Balc 31(1/2):109–110
Haydoutov I, Tenchev Y, Janev S (1979) Lithostratigraphic subdivision of the diabase–phyllitoid complex in the Berkovitsa Balkan Mountain. Geol Balk 9:13–25
Hedenquist JW, Lowenstern JB (1994) The role of magmas in the formation of hydrothermal deposits. Nature 370:519–527
Hedenquist JW, Arribas Jr A, Reynolds TJ (1998) Evolution of an intrusion-centered hydrothermal system: far Southeast—Lepanto porphyry and epithermal Cu–Au deposits, Philippines. Econ Geol 93:373–404
Heinrich CA, Neubauer F (2002) Cu–Au–Pb–Zn–Ag metallogeny of the Alpine–Balkan–Carpathian–Dinaride geodynamic province. Miner Depos 37:533–540
Heinrich CA, Günther D, Audetat A, Ulrich T, Frischknecht R (1999) Metal fractionation between magmatic brines and vapor, determined by microanalysis of fluid inclusions. Geology 27:755–758
Hill IG, Worden RH, Meighan IG (2000) Yttrium: the immobility–mobility transition during basaltic weathering. Geology 28:923–926
Ivanov Z (1989) Structure and tectonic evolution of central parts of the Rhodope massif. In: Ivanov Z (ed) Structure and geodynamic evolution of the inner zones of Balkanides—Kraishtides and Rhodope area. Guide for excursion, XIV Congress CBGA, Sofia, Bulgaria, pp 56–92
Ivanov Z, Henry B, Dimov D, Georgiev N, Jordanova D, Jordonova N (2001) New model for Upper Cretaceous magma emplacement in the southwestern parts of Central Srednogorie—petrostructural and AMS data. Rom J Miner Depos 79:60
Jacquat S (2003) Etude paragénétique et géochimique du gisement épithermal d'or et de cuivre de type "High-Sulfidation" de Chelopech, Bulgarie. M.Sc. thesis, University of Geneva (in French)
Jankovic S (1997) The Carpatho–Balkanides and adjacent area: a sector of the Tethyan Eurasian metallogenic belt. Miner Depos 32:426–433
Jelev V, Antonov M, Arizanov A, Arnaudova R (2003) On the genetic model of Chelopech volcanic structure (Bulgaria). 50 years. Ann Univ Min Geol, Geol Geophysics, Sofia 46:47–51
Kalaidjiev S, Hadjiiski G, Angelkov K (1984) Structural conditions for localization of the porphyry copper deposit Elatsite. Rev Bulg Geol Soc 45:189–196

Kamenov BK, von Quadt A, Peytcheva I (2002) New insight into petrology, geochemistry and dating of the Vejen pluton, Bulgaria. Geochem Miner Petrol 39:3–25

Kamenov B, Peytcheva I, von Quadt A (2003a) New petrological, geochemical and isotopic data bearing on the genesis of Capitan Dimitrievo pluton, Central Srednogorie, Bulgaria. In: Neubauer F, Handler R (eds) Final ABCD–GEODE 2003 workshop, Seggauberg, Austria, 22–24 March 2003, p 31

Kamenov B, Nedialkov R, Yanev Y, Stoykov S (2003b) Petrology of the Late Cretaceous ore—magmatic centres in the Central Srednogorie, Bulgaria. In: Bogdanov K, Strashimirov S (eds) Cretaceous porphyry epithermal systems of the Srednogorie zone, Bulgaria. Soc Econ Geol Guidebook 36:27–46

Kamenov B, Yanev Y, Nedialkov R, Moritz R, Peytcheva I, von Quadt A, Stoykov S, Zartova A (2004) An across-arc petrological transect trough the Central Srednogorie Late Cretaceous magmatic centers in Bulgaria. Bulgarian geological society, annual scientific conference, "geology 2004," pp 35–37

Katskov N, Iliev K (1993) Panagyurishte map sheet. In: Explanatory note to the geological map of Bulgaria in scale 1:100000, 53 pp (in Bulgarian)

Krogh TE (1973) A low-contamination method for hydrothermal decomposition of zircon and extraction of U and Pb for isotopic age determination. Geochim Cosmochim Acta 37:485–494

Le Maître RW (1989) A classification of igneous rocks and glossary of terms. Blackwell Sciences, Oxford, p 193

Lilov P, Chipchakova S (1999) K–Ar dating of the Upper Cretaceous magmatic rocks and hydrothermal metasomatic rocks from the Central Srednogorie. Geochem Miner Petrol 36:77–91 (in Bulgarian)

Lips ALW (2002) Correlating magmatic–hydrothermal ore deposit formation over time with geodynamic processes in SE Europe. In: Blundell DJ, Neubauer F, von Quadt A (eds) The timing and location of major ore deposits in an evolving orogen, Geol Soc London Spec Publ 204:69–79

Lips ALW, Herrington RJ, Stein G, Kozelj D, Popov K, Wijbrans JR (2004) Refined timing of porphyry copper formation in the Serbian and Bulgarian portions of the Cretaceous Carpatho–Balkan belt. Econ Geol 99:601–609

Losada-Calderòn AJ, McPhail DC (1996) Porphyry and high sulfidation epithermal mineralization in the Nevados del Famatina mining district, Argentina. In: Camus F, Sillitoe RM, Peterson R (eds) Andean copper deposits: new discoveries, mineralization, styles and metallogeny. Soc Econ Geol Spec Publ 5:91–118

Losada-Calderòn AJ, McBride SL, Bloom MS (1994) The geology and $^{40}Ar/^{39}Ar$ geochronology of magmatic acitivity and related mineralization in the Nevados del Famatina mining district, La Rioja province, Argentina. J South Am Earth Sci 7:9–24

Ludwig KR (1999) User's manual for Isoplot/Ex Version 2, a geochronological toolkit for Microsoft Excel. Berkeley Geochronology Center Special Publication 1a, pp 1–47

Marsh TM, Einaudi MT, McWilliams M (1997) $^{40}Ar/^{39}Ar$ geochronology of Cu–Au and Au–Ag mineralization in the Potrerillos district, Chile. Econ Geol 92:784–806

Masterman GJ, Cooke DR, Berry RF, Clark AH, Archibald AA, Mathur R, Walshe JL, Duran M (2004) $^{40}Ar/^{39}Ar$ and Re–Os geochronology of porphyry copper–molybdenum deposits and related copper–silver veins in the Collahuasi District, northern Chile. Econ Geol 99:673–690

Masterman GJ, Cooke DR, Berry RF, Walshe JL, Lee AW, Clark AH (2005) Fluid chemistry, structural setting, and emplacement history of the Rosario Cu–Mo porphyry and Cu–Ag–Au epithermal veins, Collahuasi District, northern Chile. Econ Geol 100:835–862

Moev M, Antonov M (1978) Stratigraphy of the Upper Cretaceous in the eastern part of the Sturguel–Chelopech strip. Ann Univ Min Geol 23:7–30 (in Bulgarian)

Moritz R, Kouzmanov K, Petrunov R (2004) Late Cretaceous Cu–Au epithermal deposits of the Panagyurishte district, Srednogorie zone, Bulgaria. Swiss Bull Miner Petrol 84:79–99

Moritz R, Chambefort I, Georgieva S, Jacquat S, Petrunov R (2005) The Chelopech high-sulfidation epithermal Cu–Au deposit. Ore Geol Rev 27:130–131

Pearce JA (1982) Trace elements characteristics of lavas from destructive plate boundaries. In: Thorpe RS (ed) Andesites. Wiley, Chichester, pp 525–548

Petrunov R (1994) Mineral paragenesis and physicochemical conditions of ore-forming in the Chelopech deposit. Ph.D. thesis, Geology Institute, Sofia, p 178 (in Bulgarian)

Petrunov R (1995) Ore mineral paragenesis and zoning in the deposit of Chelopech. Geochem Mineral Petrol 30:89–98 (in Bulgarian)

Petrunov R, Dragov P (1993) PGE and gold in the Elatsite porphyry copper deposit, Bulgaria. In: Fenoll Hach-Ali P, Torres-Ruiz J, Gervilla F (eds) Current research in geology applied to ore deposit, University of Granada, Granada Spain, pp 543–546

Peytcheva I, von Quadt A (2003) U–Pb–zircon isotope system in mingled and mixed magmas: an example from Central Srednogorie, Bulgaria. Geophy Res Abstr 5:09177

Peytcheva I, von Quadt A (2004) The Paleozoic protoliths of Central Srednogorie, Bulgaria: records in zircons from basement rocks and Cretaceous migmatites. 5th International symposium on eastern Mediterranean geology, Thessaloniki, Greece, extended abstract T11-9

Peytcheva I, von Quadt A, Kamenov B, Ivanov Z, Georgiev N (2001) New isotope data for Upper Cretaceous magma emplacement in the southern and south-western parts of Central Srednogorie. In: ABCD–GEODE 2001 workshop, Vata Bai, Romania, abstract volume 79(2):82–83

Peytcheva I, von Quadt A, Kouzmanov K, Bogdanov K (2003) Elshitsa and Vlaykov Vruh epithermal and porphyry Cu(–Au) deposits of Central Srednogorie, Bulgaria : source and timing of magmatism and mineralization. In: Elioupoulos DG et al (eds) Mineral exploration and sustainable development. Proceedings, 7th biennial SGA meeting, Athens, Greece, 24–28 August 2003, Millpress, Rotterdam, pp 371–373

Peytcheva I, von Quadt A, Frank M, Nedialkov R, Kamenov B, Heinrich C (2004) Timing and magma evolution of Upper Cretaceous rocks in Medet Cu–porphyry deposit: isotope–geochronological and geochemical constraints. Bulgarian geological society, annual scientific conference, "geology 2004," pp 57–59

Popov K (2001) Geology of the southern part of the Panagyurishte ore region. Ann Univ Min Geol 43–44:51–63

Popov P, Kovachev V (1996) Geology, composition and genesis of the ore mineralization in the central part of the Elatsite–Chelopech ore field. Proceeding of the annual meeting, UNESCO–ICGP Project 356, plate tectonic aspects of the Alpine metallogeny in the Carpatho–Balkan region, Sofia 1:159–170

Popov P, Popov K (1997) Metallogeny of the Panagyurishte ore region. In: Romic K, Konzulovic R (eds) Symposium "ore deposits exploration" proceedings, Belgrade, pp 327–338

Popov P, Popov K (2000) General geologic and metallogenic features of the Panagyurishte ore region. In: Strashimirov S, Popov P (eds) Geology and metallogeny of the Panagyurishte ore region (Srednogorie zone, Bulgaria), ABCD–GEODE 2000 workshop, guide book to excursions, Sofia, pp 1–7

Popov P, Petrunov R, Strashimirov S, Kanazirski M (2000) Elatsite–Chelopech ore field. In: Strashimirov S, Popov P (eds) Geology and metallogeny of the Panagyurishte ore region (Srednogorie zone, Bulgaria), ABCD–GEODE 2000 workshop, guide book to excursions, Sofia, pp 8–18

Popov P, Radichev R, Dimovski S (2001) Geology and evolution of the Elatzite–Chelopech porphyry–copper—massive sulfide ore field. Ann Univ Min Geol 43–44:31–44 (in Bulgarian)

Rohrlach BD (2003) Tectonic evolution, petrochemistry, geochronology and palaeohydrology of the Tampakan Porphyry and high-sulfidation epithermal Cu–Au deposit, Mindanao, Philippines. Ph.D. thesis, Australian National University, p 499, 23 app

Setterfield TN, Musset AE, Oglethorpe RDJ (1992) Magmatism and associated hydrothermal activity during the evolution of the Tavua Caldera: $^{39}Ar/^{40}Ar$ dating of the volcanic, intrusive, and hydrothermal events. Econ Geol 47:1130–1140

Sillitoe RH (1997) Characteristics and controls of the largest porphyry copper–gold and epithermal gold deposits in the circum-Pacific region. Aust J Earth Sci 44:373–388

Sillitoe RH (1999) Styles of high-sulfidation gold, silver and copper mineralisation in porphyry and epithermal environments. In: Weber G (ed) Proceedings, Aust Inst Mineral Metallo, PacRim'99, Bali, Indonesia, 10–13 October, pp 29–44

Stanisheva-Vassileva G (1980) The Upper Cretaceous magmatism in Srednogorie zone, Bulgaria: a classification attempt and some implications. Geol Balk 10:15–36

Stoykov S, Pavlishina P (2003) New data for Turonian age of the sedimentary and volcanic succession in the southeastern part of Etropole Stara Planina Mountain, Bulgaria. Comptes Rendus Bulg Acad Sciences 56:55–60

Stoykov S, Yanev Y, Moritz R, Katona I (2002) Geological structure and petrology of the late cretaceous Chelopech volcano, Srednogorie magmatic zone. Geochem Miner Petrol 39:27–38

Stoykov S, Yanev Y, Moritz R, Fontinie D (2003) Petrology, Sr and Nd isotope signature of the Late Cretaceous magmatism in the southeastern part of the Etropole Stara Planina, Srednogorie magmatic zone. 50 years Ann Univ Min Geol "St Ivan Rilski," 46:161–166

Stoykov S, Peytcheva I, von Quadt A, Moritz R, Frank M, Fontignie D (2004) Timing and magma evolution of the Chelopech volcanic complex (Bulgaria). Swiss Bull Miner Petrol 84:101–117

Strashimirov S, Petrunov R, Kanazirski M (2002) Porphyry–copper mineralization in the Central Srednogorie zone, Bulgaria. Miner Depos 37:587–598

Sun SS, McDonough WF (1989) Chemical and isotopic systematic of oceanic basalts: implications for mantle composition and processes. In: Saunders AD, Norry MJ (eds) Magmatism in ocean basins, Geol Soc London Spec Publ 42:313–345

Tarkian M, Hünken U, Tokmakchieva M, Bogdanov K (2003) Precious-metal distribution and fluid inclusion petrography of the Elatsite porphyry copper deposit, Bulgaria. Miner Depos 38:261–281

Thorpe RS (1982) Andesites. Wiley, Chichester, p 724

Velichkova SH, Handler R, Neubauer F, Ivanov Z (2004) Variscan to Alpine tectonothermal evolution of the Central Srednogorie unit, Bulgaria: constraints from $^{40}Ar/^{39}Ar$ analysis. Swiss Bull Miner Petrol 84:133–151

Voldet P (1993) From neutron activation to inductively coupled plasma-atomic emission spectrometry in the determination of rare-earth elements in rocks. Trends Anal Chem 12:339–344

von Quadt A, Peytcheva I (2004) Magmatic evolution of the Cretaceous rocks within the Panagyurishte district (Central Srednogorie, Bulgaria) based on U–Pb and Hf–zircon, Nd and Sr whole rock data. Bulgarian geological society, annual scientific conference, "geology 2004," pp 60–62

von Quadt A, Peytcheva I, Kamenov B, Fanger L, Heinrich C, Frank M (2002) The Elatsite porphyry copper deposit in the Panagyurishte ore district, Srednogorie zone, Bulgaria: U–Pb zircon geochronology and isotope–geochemical investigations of magmatism and ore genesis. In: Blundell DJ, Neubauer F, von Quadt A (eds) The timing and location of major ore deposits in an evolving orogen, Geol Soc London Spec Publ 204:119–135

von Quadt A, Peytcheva I, Cvetkovic V (2003) Geochronology, geochemistry and isotope tracing of the Cretaceous magmatism of East-Serbia and Panagyurishte district (Bulgaria) as part of the Apuseni–Timok–Srednogorie metallogenic belt in Eastern Europe. In: Elioupolos DG et al (eds) Mineral exploration and sustainable development, Proceedings, 7th biennial SGA meeting, Athens, Greece, 24–28 August 2003, Millpress, Rotterdam, pp 407–410

von Quadt A, Moritz R, Peytcheva I, Heinrich C (2005a) Geochronology and geodynamics of Upper Cretaceous magmatism and Cu–Au mineralization in the Panagyurishte region of the Apuseni–Banat–Timok–Srednogorie belt (Bulgaria). Ore Geol Rev 27:95–126

von Quadt A, Peytcheva I, Fanger L, Heinrich CA (2005b) The Elatsite porphyry Cu–Au deposit, Bulgaria. Ore Geol Rev 27:128–129

Winchester JA, Floyd PA (1977) Geochemical discrimination of different magma series and their differentiation products using immobile elements. Chem Geol 20:325–343

Zagorchev I, Moorbath S (1987) Rubidium–strontium isotopic data for Vitosa Pluton, Srednogorie zone. Geol Balc 13:43–48

Zimmerman A, Stein H, Markey R, Fanger L, Heinrich C, von Quadt A, Peytcheva I (2003) Re–Os ages for the Elatsite Cu–Au deposit, Srednogorie zone, Bulgaria. In: Elioupoulos DG et al (eds) Mineral exploration and sustainable development. Proceedings, 7th biennial SGA meeting, Athens, Greece, 24–28 August 2003, Millpress, Rotterdam, pp 1253–1256